ARC SPIRT Project

EXPLORATION FOR TIGHT GAS RESERVOIRS ENHANCED BY NATURAL FRACTURING, COOPER BASIN, SOUTH AUSTRALIA

Collaborators:

Santos Ltd
LDG Task Force

And

NCPGG
University of Adelaide

Scott Mildren, Peter van Ruth, Suzanne Barr and Richard Hillis

Year 2 Final Report
(12th February 2001)

Executive Summary

This ARC SPIRT project aims to identify where natural fractures enhance reservoir permeability in the 'tight' gas reservoirs of the Nappamerri Trough. Year 2 of the project, reported herein, focuses on natural fracture "sweet spot" prediction with respect to the in situ stress field.

- The Cooper Basin Stress Map illustrates a consistent ≈ 100ºN σ_{Hmax} orientation in the Nappamerri Trough and rotates to ≈ 140ºN north of the GMI structural trend (Brolga-3, Moorari-7 and Woolkina-1). Southwest of the Moomba Field are several low quality σ_{Hmax} orientations ≈ 130ºN (Farina-2, Koree South-1 and Daralingie-10).

- Pore pressure values range between 0.5 and 0.7 psi/ft across the Cooper Basin and are greatest in the Nappamerri Trough.

- Vertical stress gradients range between 0.9 and 1.0 psi/ft and are greatest in the Nappamerri Trough.

- Lower σ_{hmin} estimates are observed on the peripheries of the Nappamerri Trough.

- There is an increase in σ_{Hmax} magnitude from SW to NE across the Nappamerri Trough

- The Cooper Basin stress regime is on the boundary of strike-slip and thrust.

- The dominant natural fracture strike direction is 139°N and the mean dip magnitude is 60° to the NE and SW.

- The greatest fracture densities corrected for image coverage occur in wells adjacent to the GMI trend and in the Moomba area.

- The most fractured stratigraphic units are the Pre-Permian Basement, Wallumbilla Formation, Tirrawarra Conglomerate, Merrimelia Formation and Birkhead Formation in order of decreasing fracture density.

- Fractures dipping > 60° and striking NW-SE or ENE-WSW have the greatest fracture susceptibility and sub-vertical fractures striking N-S have the least fracture susceptibility.

- The greatest potential for exploiting hydraulically conductive natural fractures is at depth in the Nappamerri Trough, possibly towards the northern margin, in the sediments of the Warburton Basin.

- The overpressured sediments in the Nappamerri Trough are not in hydraulic communication and thus must be compartmentalized;

- The origin of overpressure is not related to hydrocarbon buoyancy unless each of the overpressured compartments has large down dip hydrocarbon columns, and;

- a Microsoft Access "Result Database" is included providing a single resource for all project analyses and related information.

Table of Contents

Status of Deliverables For End of Year 2 (2000)

AS OF 12th February 2001

DELIVERABLE	STATUS AS OF 12th FEBRUARY 2001
Technology Transfer of Regional Structural History Phase of Project (a) Report on structural history of Cooper Basin (b) Report on trishear modeling methodology (c) Hillis and/or Flottmann presentation at LDG Forum (circa March 2000) if requested	Carry over from phase one of project (a) Flottman's core analyses have been integrated into the result database (b) Trishear modeling report completed (c) LDG Forum presentation not required
Regional In Situ Stress Overview: Compile all Existing Data and Analyse Any as Yet Unanalysed Data (eg. FMS logs) (a) Horizontal stress orientation (analysis of all processed FMS logs) (b) Vertical stress magnitude (regional checkshot velocity compilation, and density log integration for at least 10 wells in excess of those done by Santos) (c) LOP and minifracture analysis (all available) for minimum horizontal stress (d) Maximum horizontal stress bounds	Compilation of pre-existing stress interpretations (20 wells) completed. Analysis of newly acquired data: 16 image logs (FMS/FMI) and 6 paper caliper logs (SHDT) Compilation of vertical stress magnitude profiles from 12 wells and 13 additional wells analysed. LOP and Minifrac data compiled from Santos database. Maximum horizontal stress bounds constrained across the Toolachee and Patchawarra Formations. Additional fracture analyses performed on image log interpretations
Overpressure Analysis (a) Compilation of formation tests, mud weights etc. to delineate observed data on overpressure (b) Analysis of log, especially velocity signature of overpressure (c) Determination of velocity effect of overpressure and input on likelihood of its detection using seismic velocities (d) Determination of the likely lateral and vertical extent of the overpressure	Compilation of data and inclusion in Results Database. Sonic log Eaton pressure estimates for 15 wells The seismic resolution needed to delineate the velocity anomaly associated with the over pressured sediments is approximately 35 us/m.
In Situ Stress Prediction (a) 2D regional models of effect of discontinuities on in situ stress field with calibration against observed data: eg. possibility of low stress zones in the viscinity of faults (b) Relationships predicting stress in the deep Nappamerri Trough combining depth, overpressure and other relevant parameters (calibrated by observed data) (c) Models and/or observational data on pore pressure, temperature/stress coupling.	Big Lake Area Pilot Study for Year 3 of SPIRT 2D model of σ_{hmin} magnitude in the Big Lake area using UDEC software for comparison with ISIP data. Sensitivity study of model parameters.
Reporting (a) Formal progress reports at six-monthly intervals (b) Project management meetings on a quarterly basis	Six-monthly status report presented 27/8/2000 Project management meetings held on 24/3/2000 and 12/7/2000

1. Introduction

This project aims to identify where natural fractures enhance reservoir permeability in the 'tight' gas reservoirs of the Nappamerri Trough. The first phase of this project (1999) identified key events in the tectonic history of the Cooper Basin that may have contributed to the formation of natural fractures through time. The second phase of the project (2000), reported herein, focused on the vertical and aerial distribution of stress in the Nappamerri Trough and the contribution of pore pressure to the in situ stress state of the target reservoirs. These data can are used to highlight natural fracture plays or 'sweet spots' that can be exploited for hydrocarbons.

This phase of the project has concentrated on the following areas:

- stress orientations;
- the stress tensor;
- fracture analysis;
- overpressure analysis, and;
- the results database.

A pilot study of 2D numerical stress modeling has also been performed as a precursor to the final phase of the SPIRT project (2001).

This report will briefly address the progress in each of these areas and summarise the results in terms of 'sweet spot' identification. All work was conducted by Scott Mildren, Peter Van Ruth and Susanne Barr of the NCPGG, University of Adelaide, in close consultation with David Warner (Senior Staff Geologist, Santos LDG Task Force) and Richard Hillis (NCPGG, University of Adelaide).

2. Stress Orientation

In situ stress orientations were interpreted from 16 newly-analysed digital image logs (FMS/FMI/CBIL) and 6 newly-analysed paper caliper logs (HDT/SHDT). Furthermore, 20 stress orientations were compiled from pre-existing stress studies (Table 1). All digital FMS/FMI image logs were obtained directly from Schlumberger. A CBIL acoustic image log was obtained by Santos in December 2000 from Moomba-134. Mildren (2001) provided a detailed interpretation of the Moomba-134 data and the relevant observations have been incorporated into the findings of this study.

Tool	Format	Number of Wells	Data Source
Various/ Unknown	Text	20	Pre-existing internal Santos reports
FMS/FMI/CBIL	Digital	16	Schlumberger
(S)HDT	Paper	6	Santos

Table 1 Summary of image and caliper log data acquired for interpretation and compilation of stress orientations across the Cooper Basin.

The orientation of the maximum horizontal stress direction (σ_{Hmax}) is determined from stress induced borehole breakouts and drilling induced tensile fractures observed from the image and caliper data. Statistical means are calculated for individual wells using directional statistics. A summary of these results is presented in Figure 1, Enclosure 1, Table 2 and Table 3.

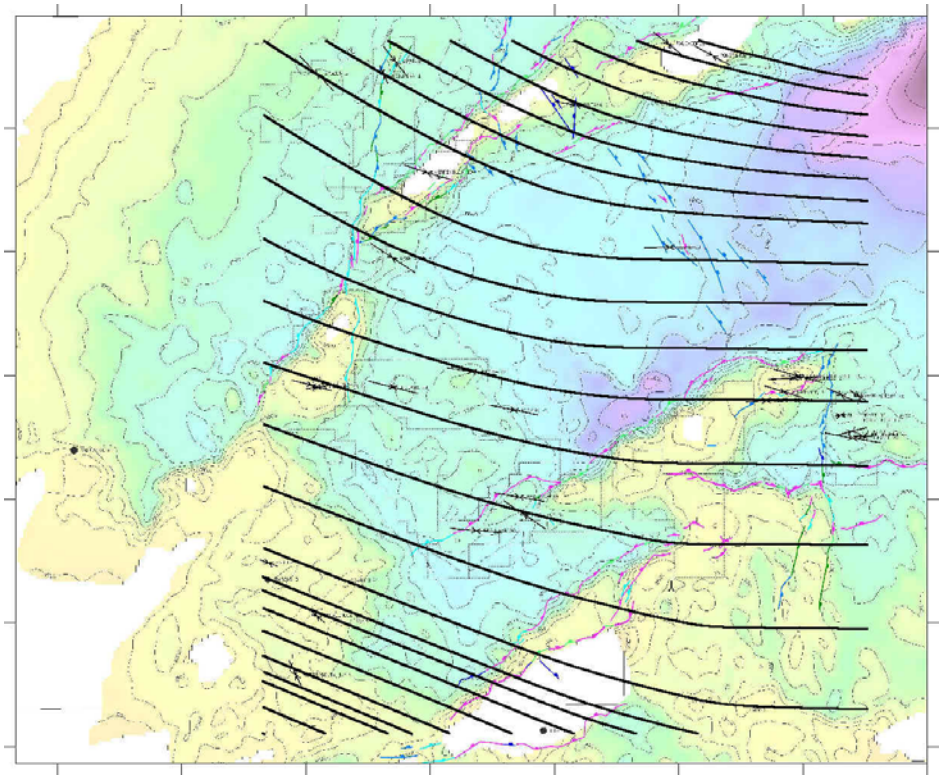

Figure 1 Maximum horizontal stress trajectories interpolated from in situ stress map of the Cooper Basin (Toolachee Formation). Long axes indicate σ_{hmax} direction and their length is weighted according to Zoback's (1992) World Stress Map ranking system.

Well Name	Lat	Long	Un-weighted				Length-weighted			Ecc-weighted		
			N	Azimuth	SD	Q	ΣL	Azimuth	SD	Q	Azimuth	SD	Q
Biala-7	28°32'	140°22'	2	105	5.0	D	1.0	105	5.0	D	No caliper information		
Brolga-3	27°35'	140°00'	45	136	6.0	A	109.8	137	5.0	A	135	4.6	A
Dullingari North-8	28°05'	140°51'	32	104	7.0	A	395.7	105	5.7	A	106	5.0	A
Dullingari-10	28°03'	140°53'	2	121	0.0	D	5.6	121	0.0	D	121	0.0	D
Dullingari-11	28°03'	140°51'	2	116	2.5	D	13.1	114	2.1	D	116	2.5	D
Dullingari-47	28°07'	140°53'	3	113	8.3	D	8.8	111	7.4	D	109	5.5	D
Koree South-1	28°27'	139°58'	3	160	8.6	D	1.1	157	6.9	D	168	7.5	D
Merrimelia-30	27°44'	140°11'	14	107	5.6	A	19.4	107	6.5	A	106	5.6	A
Merrimelia-32	27°44'	140°11'	6	114	4.7	B	20.9	114	3.1	B	114	4.9	B
Moomba-73	28°01'	140°15'	29	101	6.2	A	65.6	100	5.0	A	101	8.0	A
Moomba-74	28°02'	140°08'	7	106	2.9	B	14.1	104	2.6	B	106	3.5	B
Moomba-78	28°04'	140°19'	5	098	2.4	C	53.5	098	2.0	C	097	1.5	C
Nappacoongee-2	28°02'	140°47'	12	089	16.9	B	321.0	092	15.2	B	084	13.9	B
Swan Lake-4	27°51'	140°08'	23	123	6.8	A	161.2	124	6.2	A	No caliper information		
Wilpinnie-1	28°04'	140°44'	11	083	15.6	B	245.0	079	21.5	C	086	15.3	B
Wilpinnie-2	28°03'	140°46'	8	106	13.3	B	17.2	110	15.1	B	106	14.0	B
Yalchirrie-1	27°33'	140°35'	29	123	14.7	B	11.0	110	34.0	D	111	10.0	A
Totals			233	110	19.5	B	1463.9	099	18.6	B	095	16.7	B

Table 2 Summary of σ_{Hmax} orientation derived from newly made observations of borehole breakouts from image and caliper logs across the Cooper Basin. Lat and Long are the latitude and Longitude of the well locations N is the total number and ΣL the total length of breakouts in the well. Azimuth and SD are the mean strike (000°-180°) of breakouts in the well and their standard deviation in degrees as determined by directional statistics. Q is the quality rating of the measurement as determined using the World Stress Map ranking system (Zoback, 1992). Ecc (eccentricity) is the maximum difference between orthogonal caliper pairs.

Well Name	Lat	Long	Un-weighted			
			N	Azimuth	SD	Q
Brolga-3	27°35'	140°00'	5	141	11.3	C
Dullingari North-8	28°05'	140°51'	58	100	7.9	A
Dullingari-47	28°07'	140°53'	54	110	7.6	A
Farina-2	28°17'	139°55'	2	109	1.0	D
Gidgealpa-55	28°02'	140°00'	2	106	0.8	D
Merrimelia-30	27°44'	140°11'	12	103	30.0	D
Merrimelia-32	27°44'	140°11'	2	095	4.7	D
Moomba-73	28°01'	140°15'	14	100	12.6	B
Yalchirrie-1	27°33'	140°35'	5	127	3.7	C
Totals			154	106	14.0	B

Table 3 Summary of σ_{Hmax} orientation derived from newly made observations of drilling induced tensile fractures from image and caliper logs across the Cooper Basin. Lat and Long are the latitude and Longitude of the well locations and N is the total number of DITFs in the well. Azimuth and SD are the mean strike (000°-180°) of DITFs in the well and their standard deviation in degrees as determined by directional statistics. Q is the quality rating of the measurement as determined using the World Stress Map ranking system (Zoback, 1992).

It was originally intended to generate several stress orientation maps for separate stratigraphic horizons across the Cooper Basin. The distribution of breakouts and DITFs observed did not permit statistically significant mean orientations for individual wells to be calculated within these units. The orientation of σ_{Hmax} does vary with depth in several of the wells (Figure 2). However, these rotations are not gradual but localized adjacent to faults and/or fracture swarms. The stress map illustrated in Enclosure 1 is considered to be an accurate indication of σ_{Hmax} orientation with depth.

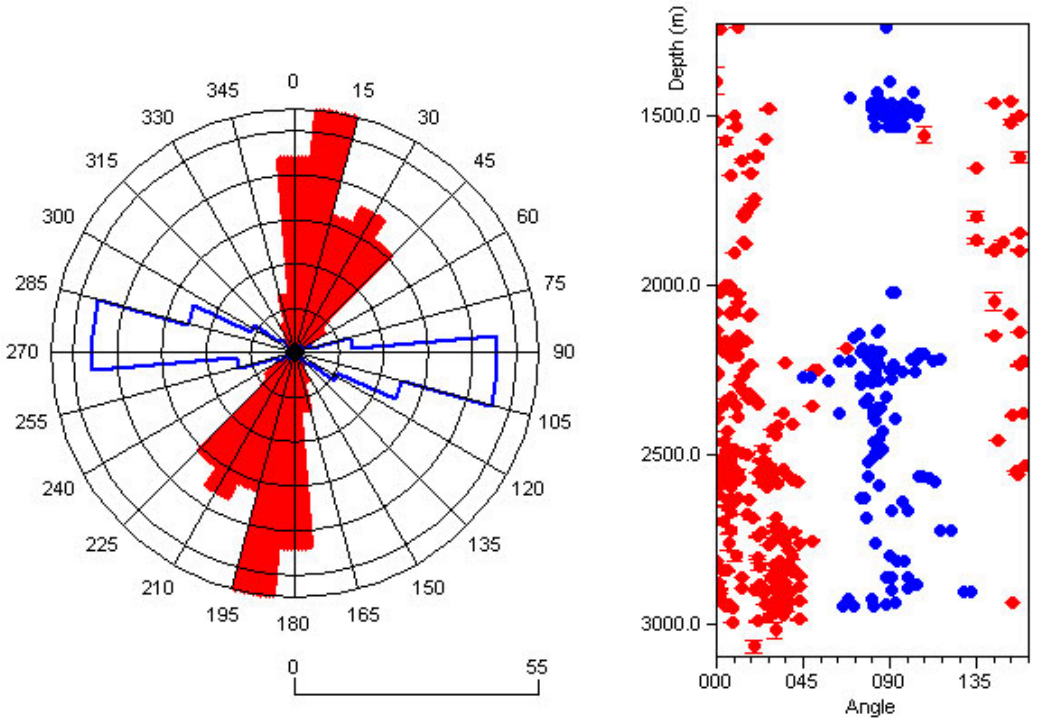

Figure 2 Summary of breakout (red) and DITF (blue) orientations in the Cooper Basin. (a) Rose diagram illustrating breakout and DITF strike directions. (b) Distribution of breakout and DITF orientation with depth.

The Cooper Basin Stress Map illustrates a consistent ≈ 100ºN σ_{Hmax} orientation within the Nappamerri Trough and rotates to approximately NW-SE north of the GMI trend (Brolga-3, Moorari-7 and Woolkina-1). Southwest of the Moomba Field are several low quality stress indicators also oriented NW-SE (Farina-2, Koree South-1 and Daralingie-10). Comparison of stress trajectories with empirical stress orientations suggests that the interpolated σ_{Hmax} orientation best fits the observed data in the Nappamerri Trough. Towards the margins of the trough the error associated with the predicted σ_{Hmax} orientation increases. Further modeling of in situ stress orientation and magnitude will become the focus of the SPIRT project in 2001.

3. Stress Tensor

A primary aim of this project was to determine the stress tensor across the Cooper Basin. Measurements were made from wells across the basin and used to extrapolate values between them. Stress magnitude is depth dependent and therefore each component was analysed and mapped over three stratigraphic horizons; the Toolachee Formation, the Patchawarra Formation and the Tirrawarra Sandstone. Contour maps were generated from data gridded using the Radial Basis Function. This function is designed for small datasets (<250 points).

The in situ stress tensor is defined using a wide range of data (Figure 3). All components of the stress tensor can be directly measured with the exception of σ_{Hmax}. The maximum horizontal stress magnitude is constrained by utilising the other components of the stress tensor to model borehole deformation. Measurement of the stress tensor is constrained to tie points (wells) where the complete suite of data was available to estimate σ_{Hmax}.

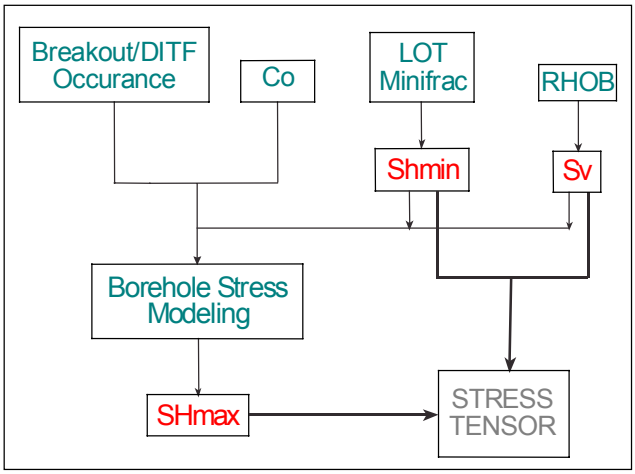

Figure 3 Flowchart illustrating component data and analyses required to generate in situ stress tensor.

Pore Pressure

There exist few direct measurements of pore pressure in the Cooper Basin. However, comparison of DST's with mudweight by van Ruth & Hillis (2000) show that they are generally consistent. Therefore, in the absence of direct pressure data mudweight has been used as a proxy for pore pressure. The distribution of pore pressure in the Cooper Basin across the Toolachee Formation., Patchawarra Formation. And Tirrawarra Sandstone are shown in Figure 4, Figure 5 and Figure 6.

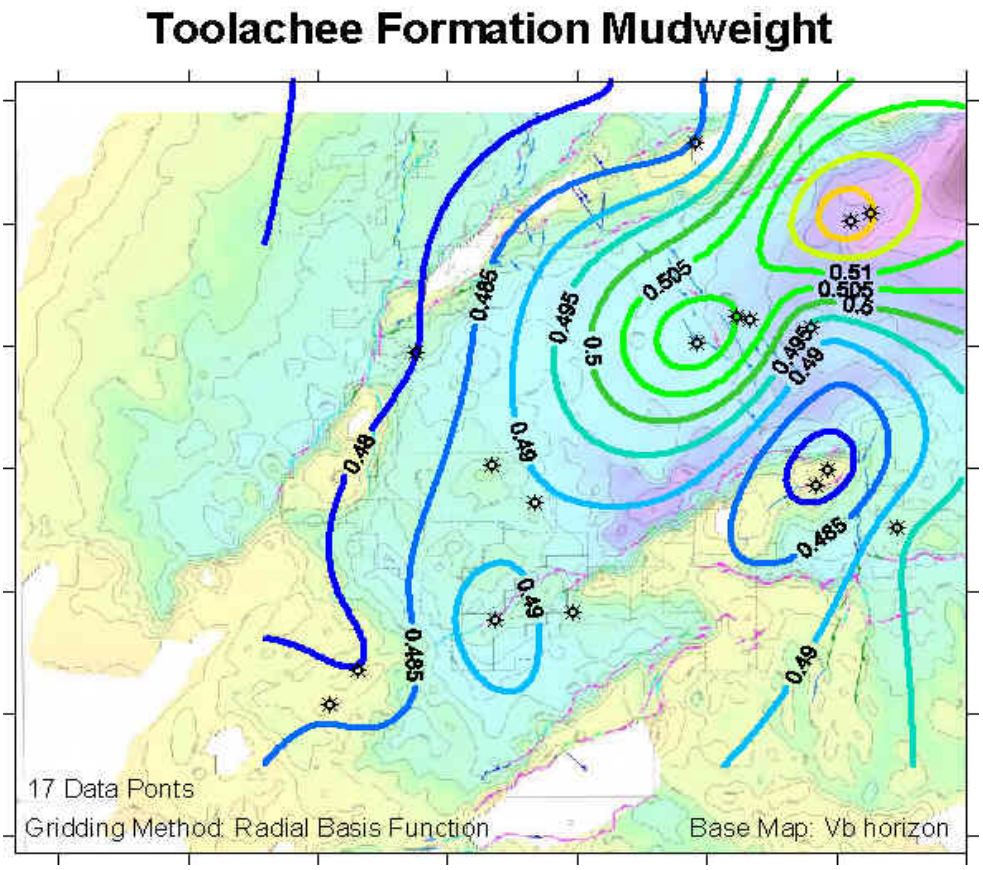

Figure 4 Toolachee Formation pore pressure gradients (psi/ft) estimated from mudweight.

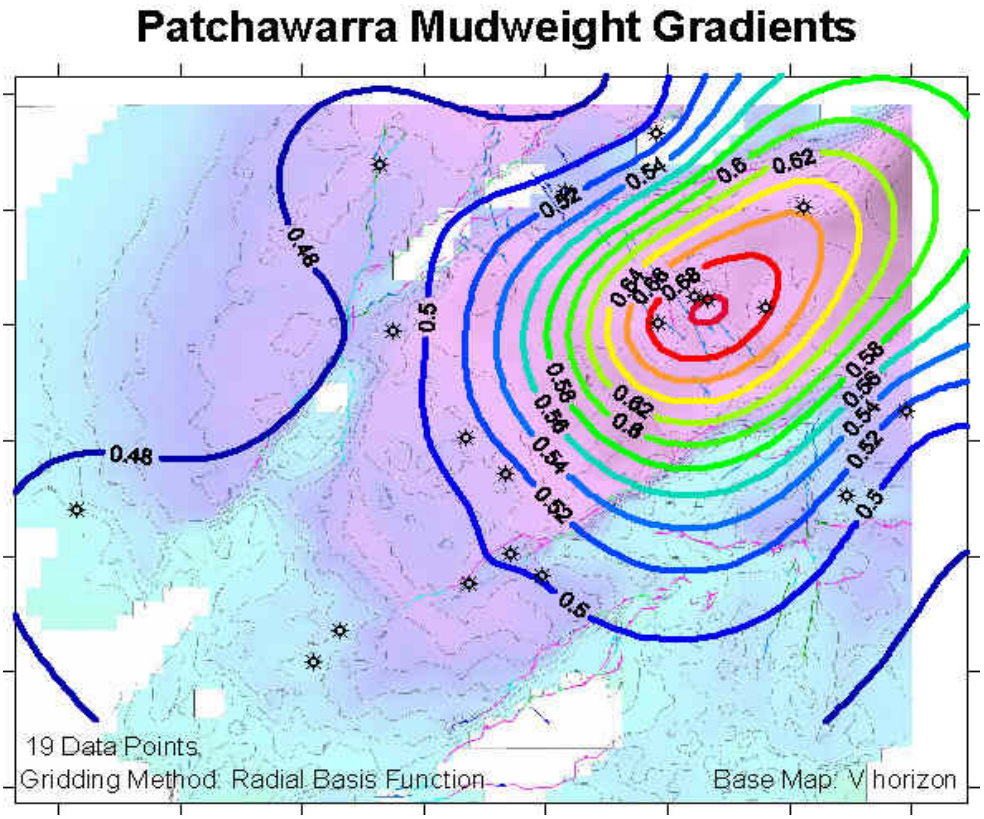

Figure 5 Patchawarra Formation pore pressure gradients (psi/ft) estimated from mudweight.

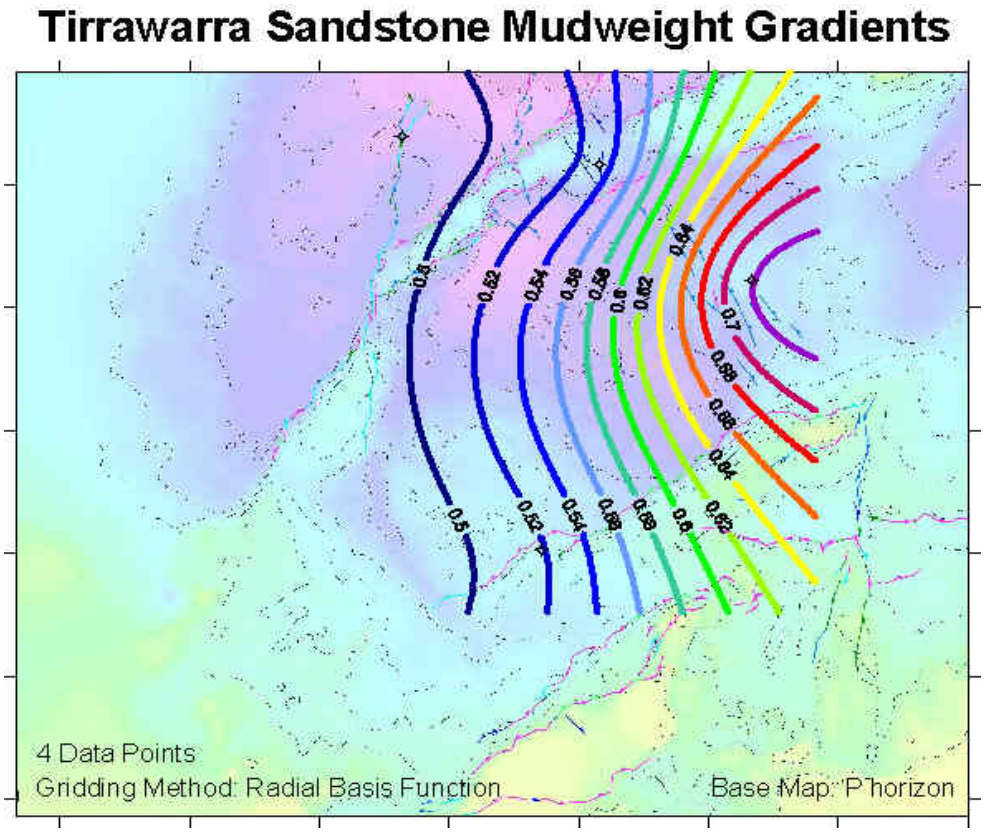

Figure 6 Tirrawarra Sandstone pore pressure gradients (psi/ft) estimated from mudweight.

The three horizon maps illustrate a consistent distribution of pore pressure across the Cooper Basin. Pressure values range between 0.5 and 0.7 psi/ft across the Basin and are greatest in the Nappamerri Trough region.

Vertical Stress Magnitudes

Calculation of the vertical stress magnitude is based on the assumption that the weight of the overburden equals the vertical stress magnitude (McGarr & Gay, 1978). This relationship can be expressed as:

$$\sigma_v = \int_z^0 \rho(z) g.dz$$

where ρ is the density of the overlying rock at depth z and g is the acceleration due to gravity. This calculation is made using density log data.

Twelve vertical stress magnitude profiles were compiled from previously made analyses (Greenstreet, 1999; Hillis, 1996) and 12 additional wells were analysed for this project (Table 4). Additional vertical stress profiles were generated using the methodology presented by Greenstreet (1999). This methodology included filtering each RHOB curve for bad hole data and applying a constant density value for intervals where coal was flagged. In addition, a Nafe-Drake transform was used to estimate density from checkshot velocities from the surface to the top of each density log. All vertical stress profiles are presented in Figure 7.

Well Name	Top Depth (m)	Bottom Depth (m)	Interpreter
Biala-1	1127.15	1593.34	S.D. Mildren
Bulyeroo-1	2330.35	3560.22	R.R. Hillis
Burley-2	244.60	3709.26	R.R. Hillis
Corkwood-1	262.47	2322.83	C. Greenstreet
Cowan-1	328.08	2378.61	C. Greenstreet
Dilchee-1	164.04	3001.97	C. Greenstreet
Dullingari North-4	1439.11	2821.69	S.D. Mildren
Fly Lake-4	1721.97	2910.38	S.D. Mildren
Gidgealpa-54st	31.24	2316.33	S.D. Mildren
Goyder-1	1279.25	2264.97	S.D. Mildren
Kirby-1	2006.50	3870.96	R.R. Hillis
Lepena-1	249.34	2437.66	C. Greenstreet
Lowanna-1	314.96	3316.93	C. Greenstreet
Malgoona-2	1873.00	2338.12	S.D. Mildren
McLeod-1	2271.52	3812.29	R.R. Hillis
Merrimelia-6	1439.27	2264.97	S.D. Mildren
Moomba-6	200.13	3028.22	C. Greenstreet
Moomba-61	2042.43	3261.13	S.D. Mildren
Mundi-1	1328.32	2461.26	S.D. Mildren
Munkarie-1	1212.04	2340.71	S.D. Mildren
Nappacoongee-2	262.47	2125.98	C. Greenstreet
Nulla-1	1622.76	2778.10	S.D. Mildren
Pondrinie-1	1349.50	2434.44	S.D. Mildren
Swan Lake-1	1759.61	3079.09	R.R. Hillis
Wantana-1	1662.84	2942.84	S.D. Mildren

Table 4 Wells for which vertical stress profiles were created or compiled.

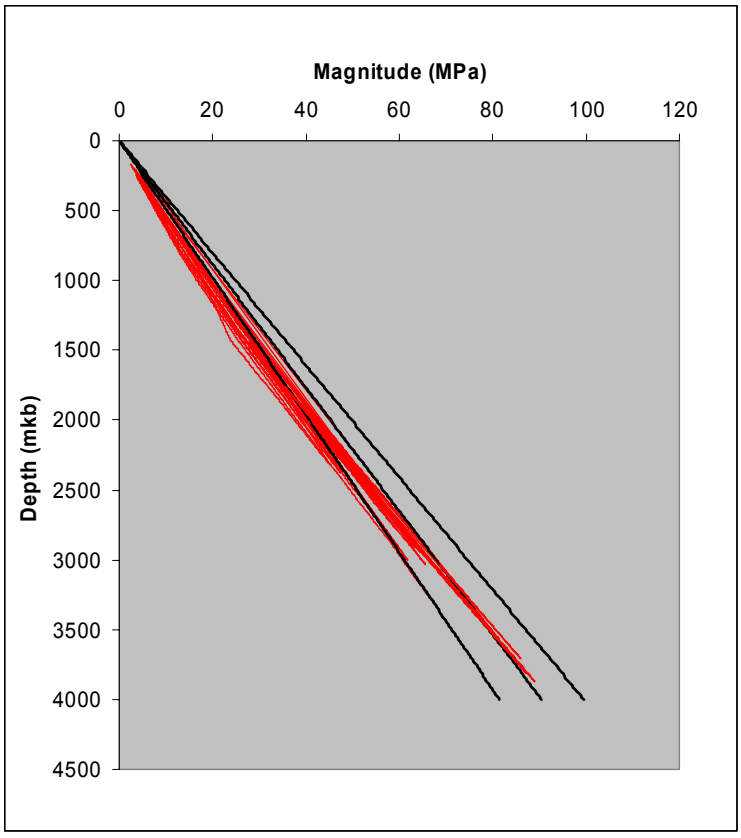

Figure 7 Vertical stress profiles calculated from Cooper Basin wells. Includes stress profiles compiled from previously existing reports (Greenstreet, 1999; Hillis, 1996)

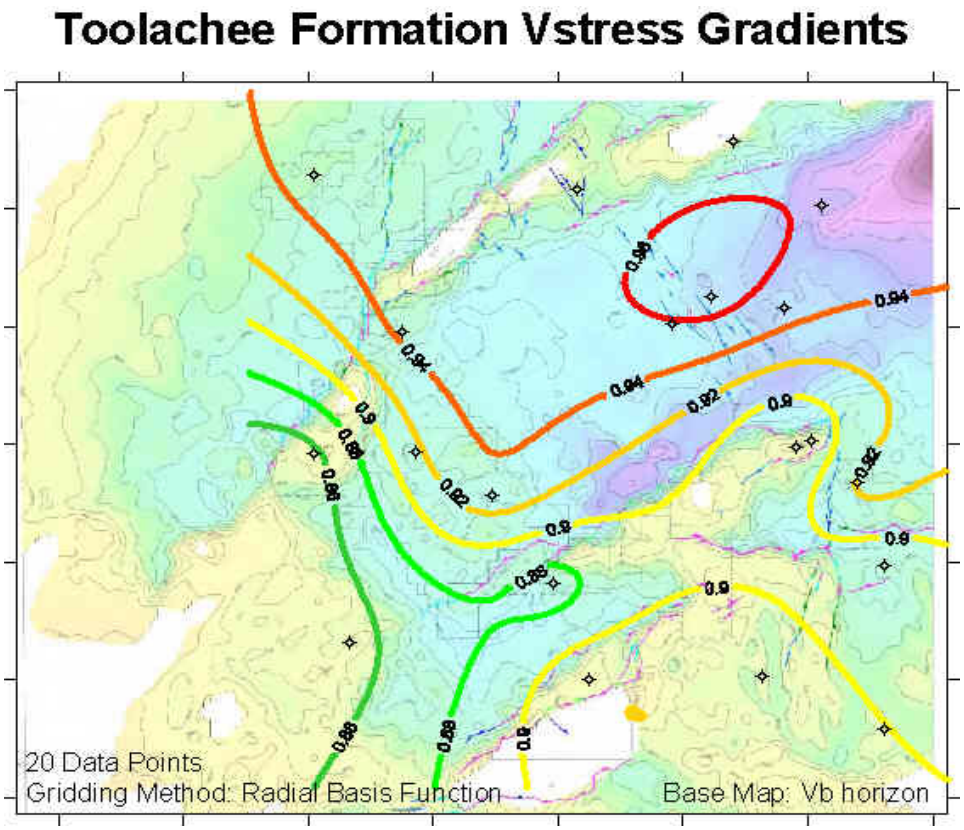

Figure 8 Toolachee Formation vertical stress gradients in psi/ft.

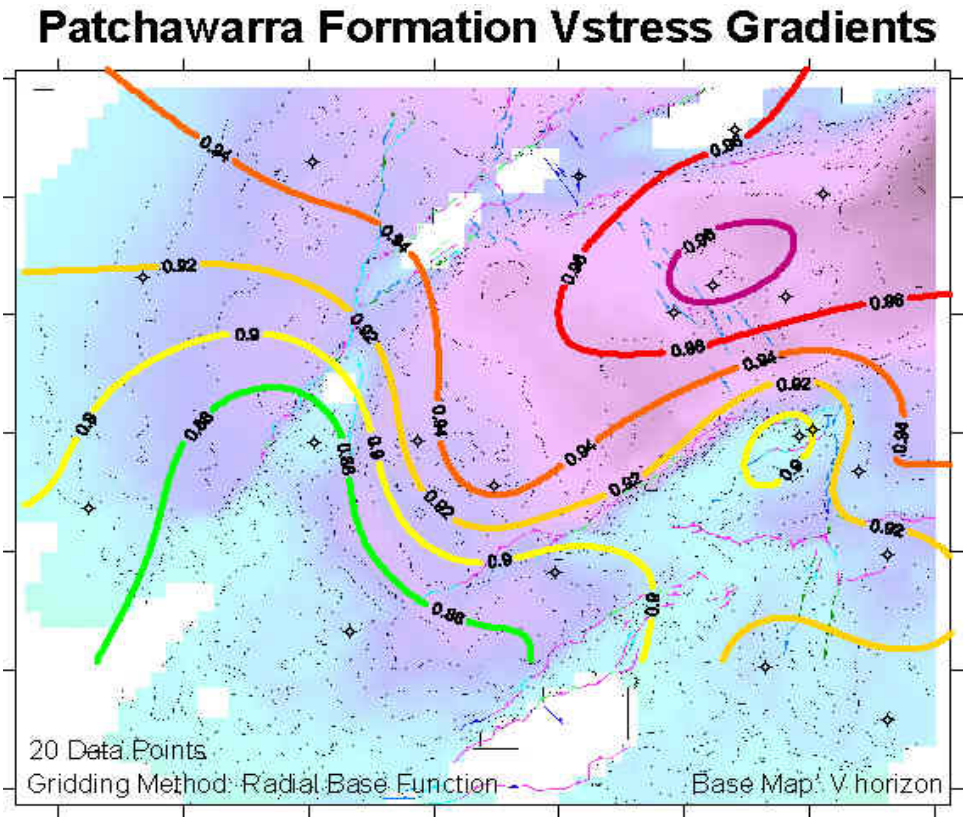

Figure 9 Patchawarra Formation vertical stress gradient in psi/ft.

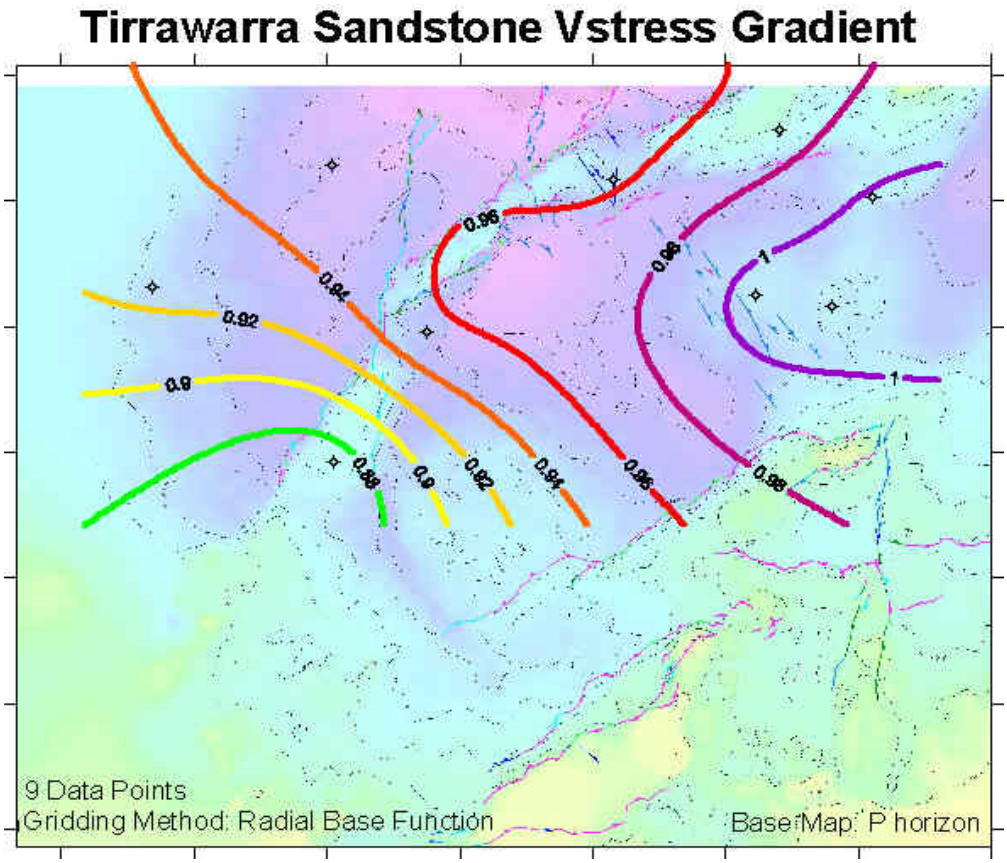

Figure 10 Tirrawarra Sandstone vertical stress gradient in psi/ft.

Horizon maps of vertical stress gradient illustrate a similar distribution of stress with depth. Each map indicates gradients ranging between 0.9 and 1.0 psi/ft. The greatest σ_v gradients are located within the Nappamerri Trough itself.

Minimum Horizontal Stress Magnitude

The minimum horizontal stress magnitude has been estimated from closure pressures recorded during minifrac tests. Each closure pressure has been sorted according to stratigraphic horizon. Contoured closure pressure gradients for each of these horizons are presented in Figure 11, Figure 12 and Figure 13.

The spread of data points varies considerably across each stratigraphic horizon. This distribution must be considered when comparing the gridded contour maps together. Although there are considerable differences between each horizon, lower estimates of σ_{hmin} magnitude are observed on the peripheries of the Nappamerri Trough compared to within the Trough itself. The area northwest of the GMI trend with is the best example of this illustrating fracture closure pressure gradients of 0.82 psi/ft or lower. Additional data may reveal a similar distribution to that observed for σ_v and mudweight.

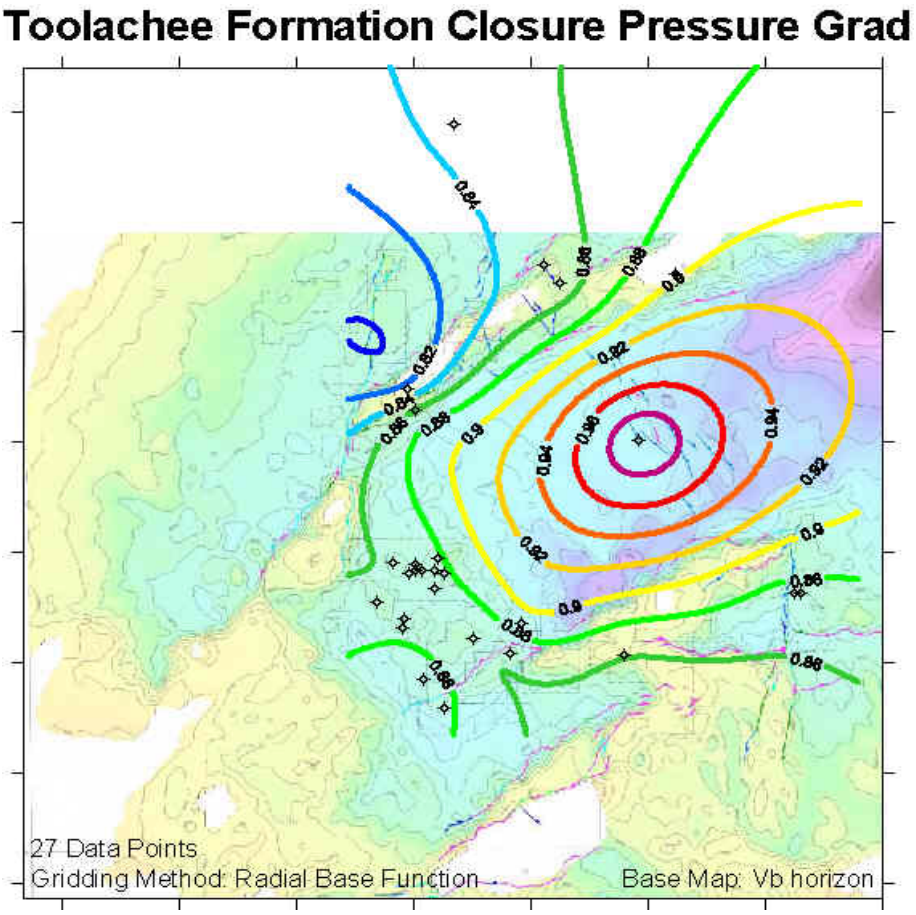

Figure 11 Toolachee Formation minifrac closure pressure gradients in psi/ft.

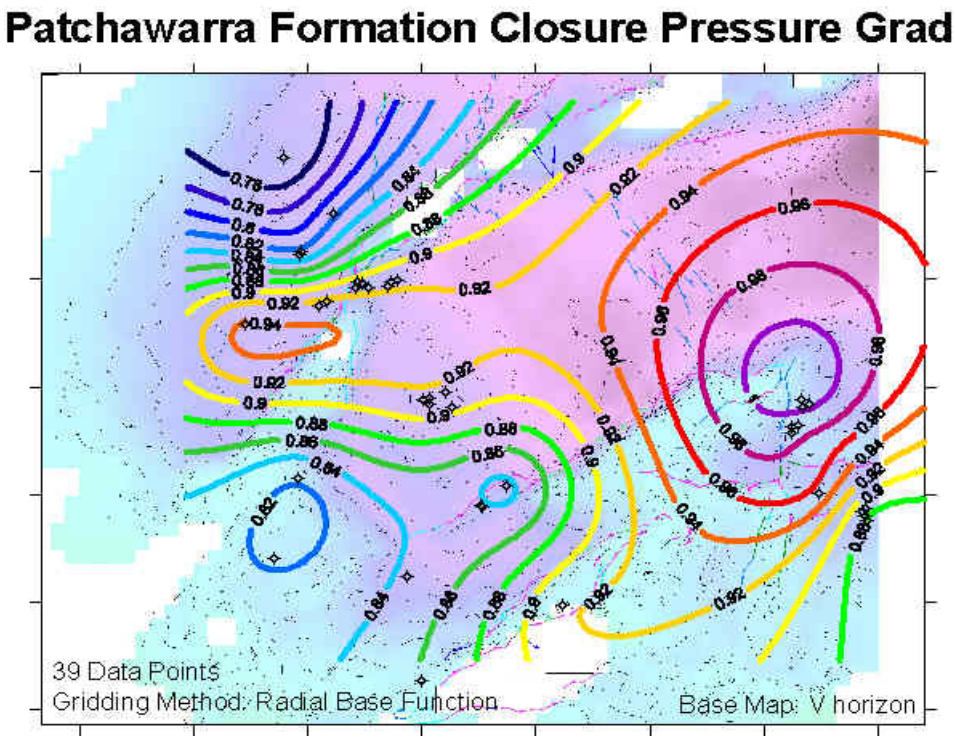

Figure 12 Patchawarra Formation minifrac closure pressure gradients in psi/ft.

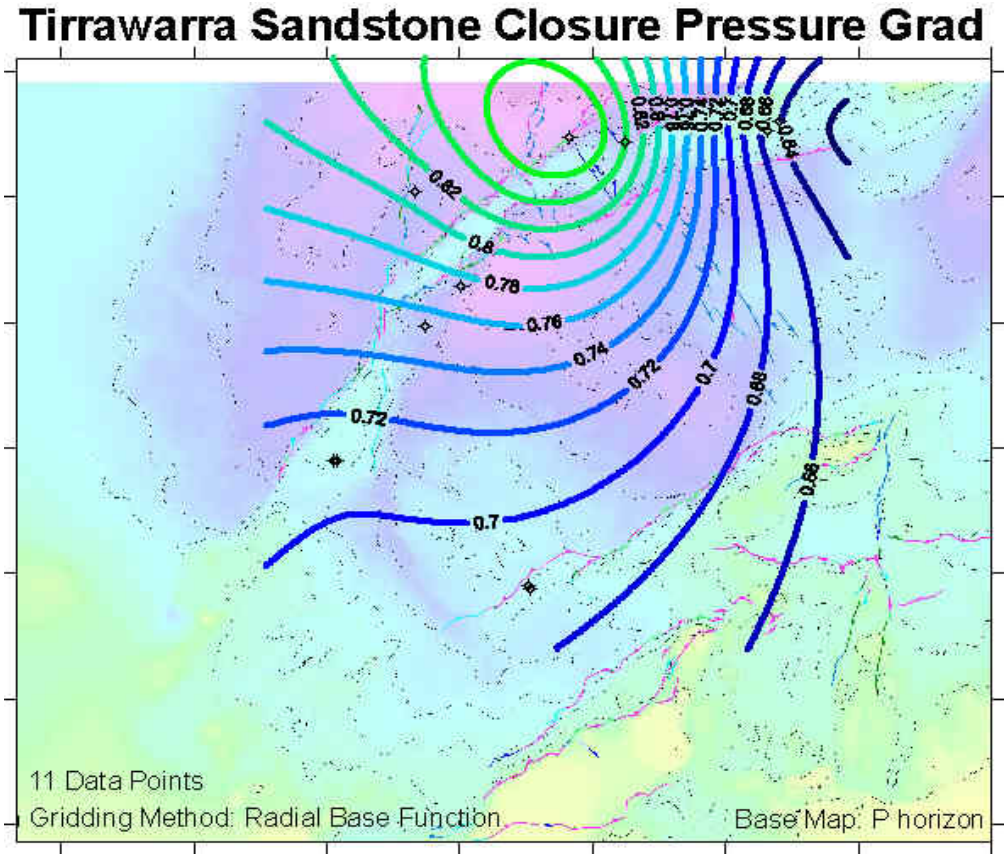

Figure 13 Tirrawarra Sandstone minifrac closure pressure gradients in psi/ft.

Maximum Horizontal Stress Magnitude

The maximum horizontal stress magnitude (σ_{Hmax}) is estimated by modeling borehole stresses to match the conditions for the occurrence and non-occurrence of breakouts and drilling induced tensile fractures (DITFs) in a wellbore. In addition, pore pressure, σ_v and σ_{hmin} magnitude are required to estimate σ_{Hmax} (Figure 3). Unconfined compressive rock strengths (UCS) were compiled from testing of the Toolachee Formation in the Barrolka Field suggesting a Co range between 150 and 300 MPa. Each σ_{Hmax} calculation was made using the software package SWIFT (Stress Wellbore Interactive Failure Tool) to interactively models σ_{Hmax} magnitude (Figure 14).

Data points are restricted to well locations where image logs are available and the occurrence and non-occurrence of breakouts is known. Full data suites were available to define the σ_{Hmax} magnitude at eight well locations in the Toolachee Formation and nine in the Patchawarra Formation. Relative stress magnitudes suggest that the Cooper Basin is on the boundary of strike-slip and thrust i.e. $\sigma_{hmin} \approx \sigma_v$ (Table 5 and Table 6). Gridded contour maps of σ_{Hmax} gradients across the Toolachee and Patchawarra Formations illustrate relatively similar distributions given the spread of data points (Figure 15 and Figure 16). Each shows an increase in gradient from the SW to NE across the Nappamerri Trough with values ranging from approximately 1.5 to 2 psi/ft.

The distribution of stress across the Cooper Basin has implications for natural fracture 'sweetspot' detection. The relation ship between natural fractures and the in situ stress tensor wil be considered in the following chapter, Fracture Analysis.

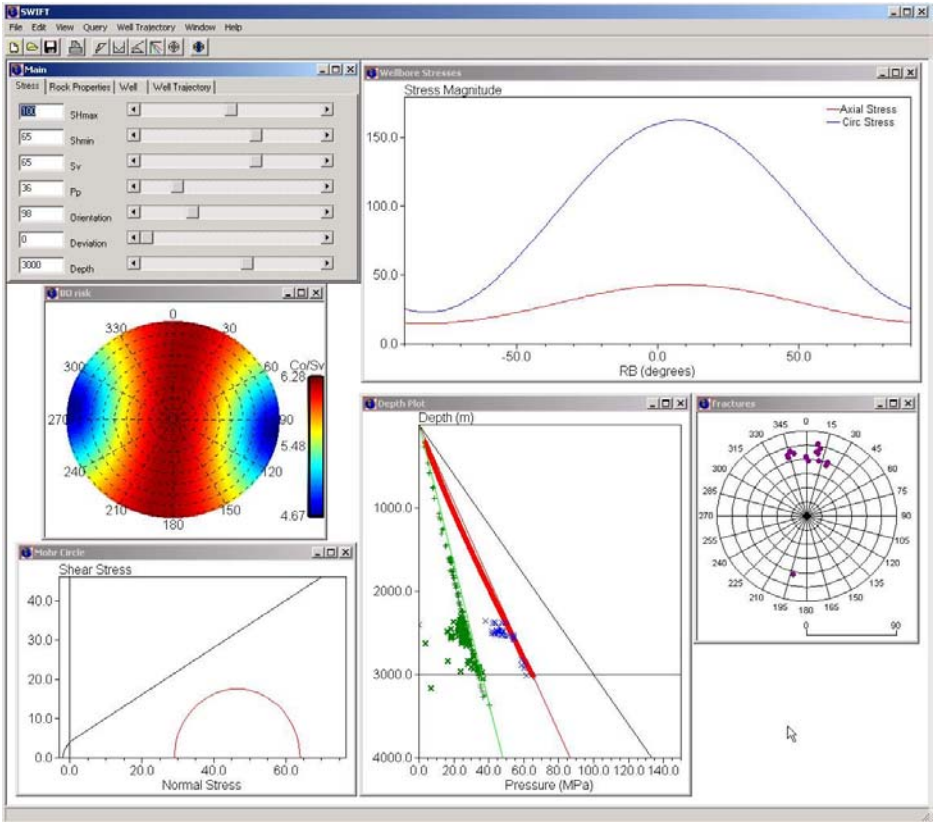

Figure 14 Screenshot from SWIFT illustrating how borehole stresses are modeled to replicate observed stress indicators and determine σ_{Hmax} magnitude.

Well Name	Easting	Northing	σv	σHmax	σhmin	Pp
Big Lake-27	434308.5	6880429	1	1.8	0.97	0.57
Big Lake-30	427407	6875170	1	1.9	1	0.56
Big Lake-54	435172.9	6877609	1	2	1	0.56
Moomba-73	426828.3	6900596	1	1.9	0.94	0.51
Moomba-74	414279	6898078	1	1.6	0.89	0.52
Moomba-78	433472.8	6894391	1	1.9	0.98	0.51
Nappacoongee East-1	478490.3	6899843	1	2.1	1	0.54
Bulyeroo-1	458372.1	6920503	1	2	1	0.55

Table 5 Stress magnitude ratios at well locations in the Toolachee Formation relative to σ_v.

Well Name	Easting	Northing	σv	σHmax	σhmin	Pp
Barina-2	394013	6867275	1	1.3	0.98	0.56
Big Lake-27	434308.5	6880429	1	1.6	0.90	0.58
Big Lake-30	427407	6875170	1	1.9	1.00	0.58
Big Lake-54	435172.9	6877609	1	1.9	0.97	0.58
Moomba-73	426828.3	6900596	1	2.0	0.99	0.54
Moomba-74	414279	6898078	1	1.8	0.97	0.54
Moomba-78	433472.8	6894391	1	1.8	0.96	0.53
Nappacoongee East-1	478490.3	6899843	1	2.0	1.00	0.60
Swan Lake-1	414935.4	6919020	1	2.1	1.00	0.52

Table 6 Stress magnitude ratios at well locations in the Patchawarra Formation relative to σ_v.

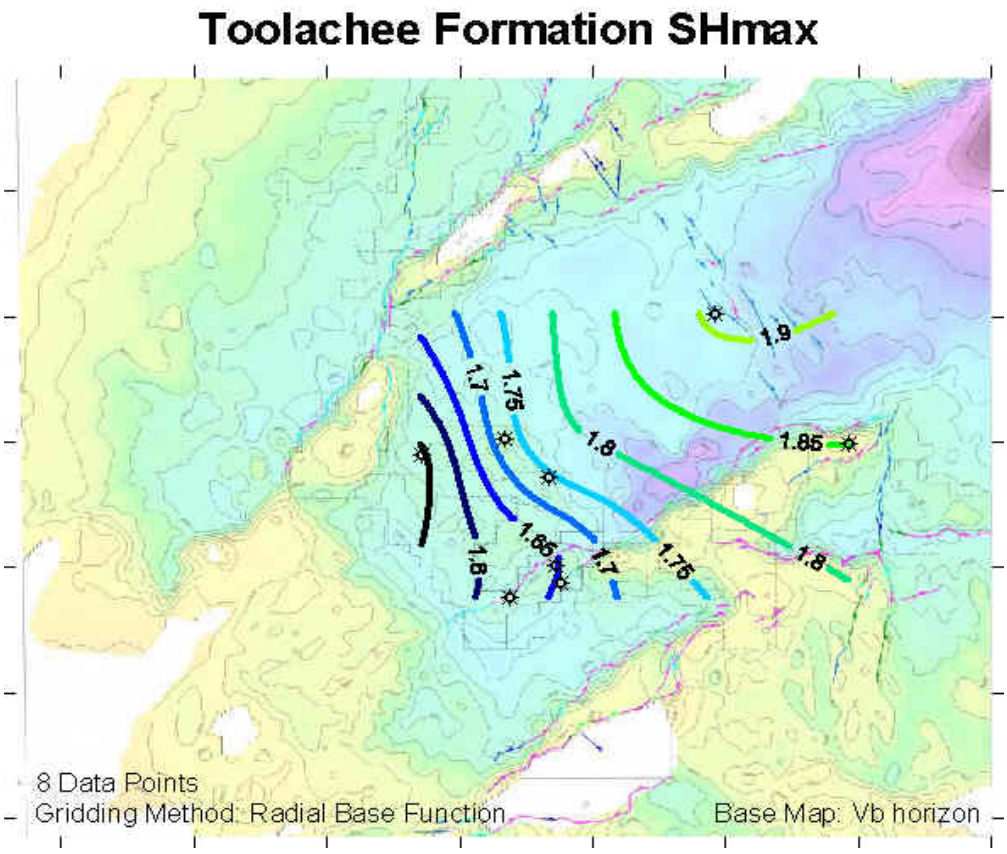

Figure 15 Toolachee Formation maximum horizontal stress gradients in psi/ft.

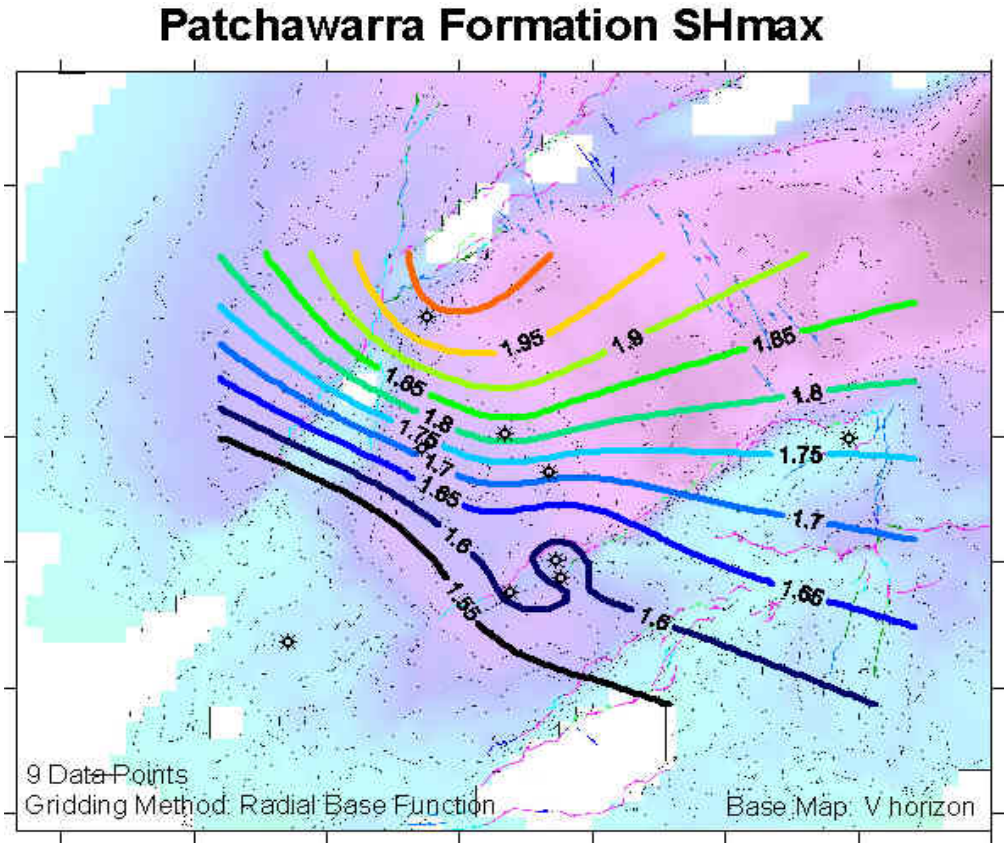

Figure 16 Patchawarra Formation maximum horizontal stress gradients in psi/ft.

4. Fracture Analysis

The aim of the fracture analysis was to assess the distribution of fractures observed in image logs from the Cooper Basin. The fracture distribution can then be integrated with the in situ stress conditions to make predictions regarding the occurrence of natural fracture 'sweet spots' within the basin. The likelihood of open, hydraulically conductive, natural fractures is predicted using a concept known as fracture susceptibility.

Fracture Distribution

In addition to observing stress induced phenomena from image logs natural fractures were also interpreted. In total 348 conductive fractures and 79 resistive fractures were observed within 18309 ft of image log. The distributions of conductive and resistive fractures are similar with directional statistics indicating mean strike directions less than 20° apart and a mean dip angle of 60° in each case. The distribution of conductive and resistive fractures is illustrated in Figure 17, Figure 18 and Figure 19. Low amplitude fractures interpreted from the acoustic images (acquired by the CBIL tool) are treated equivalent to conductive fractures in all figures and text.

Raw fracture densities have been calculated for each well and normalised for image coverage (Table 7; Figure 20). The greatest populations of conductive and resistive fractures are located in wells adjacent to the GMI trend and in the Moomba area. There are also good fracture densities in wells southwest of Moomba (Barina-2 and Biala-7). In addition, fracture density calculations have been made by formation and normalised for image coverage (Table 8; Figure 21). These data indicate that the greatest fracture populations exist within the Pre-Permian sediments, Wallumbilla Formation, Tirrawarra Conglomerate, Merrimelia Formation and Birkhead Formation in order of decreasing fracture density. In particular, the fracture density calculated for the Pre Permian sediments is almost double that of all other stratigraphic units.

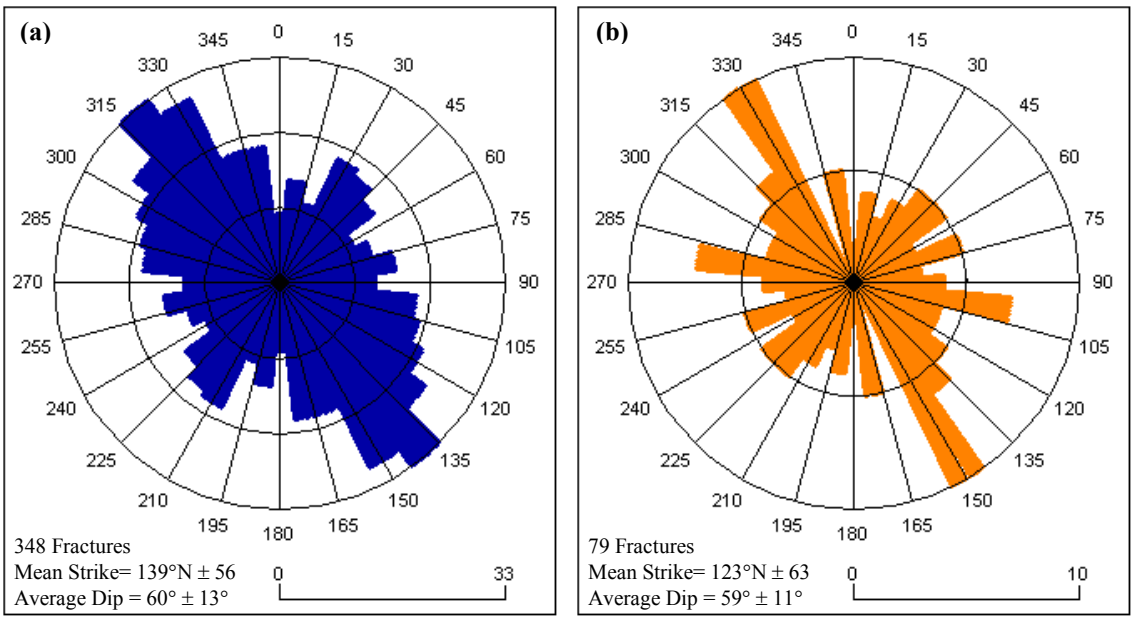

Figure 17 Strike rose diagrams of (a) conductive fractures and (b) resistive fractures interpreted from image logs in the Cooper Basin.

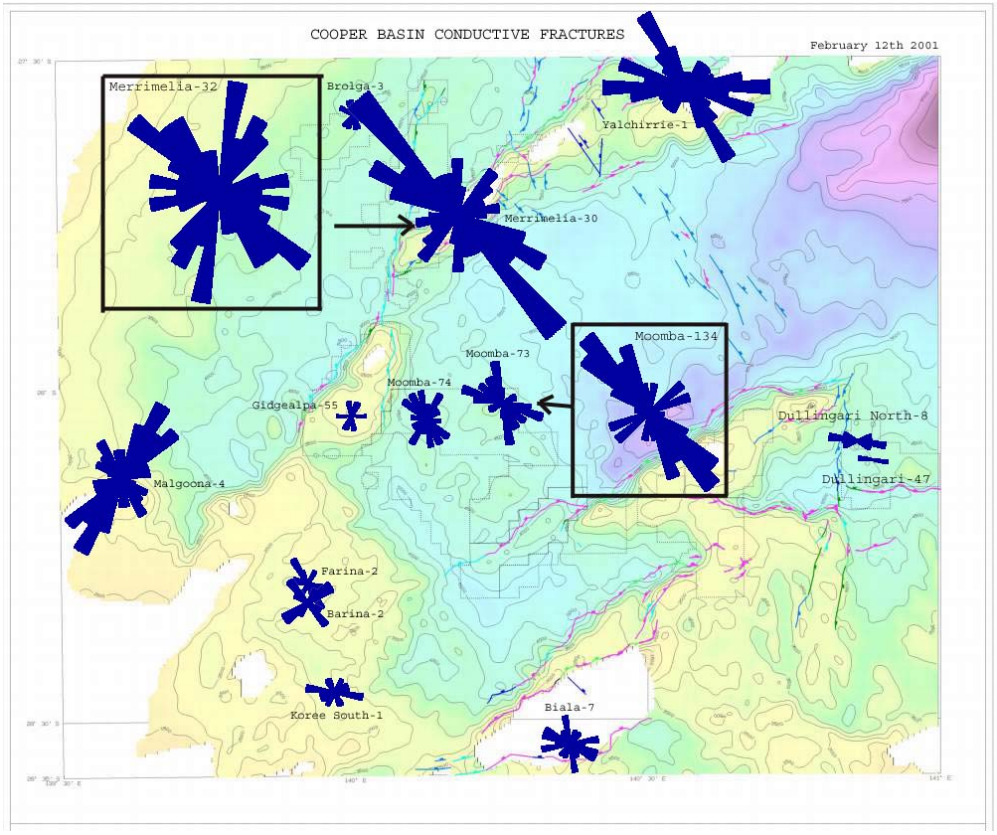

Figure 18 Map of conductive fracture distributions interpreted from resistivity logs in the Cooper basin. Rose petals are length weighted relative to fracture numbers.

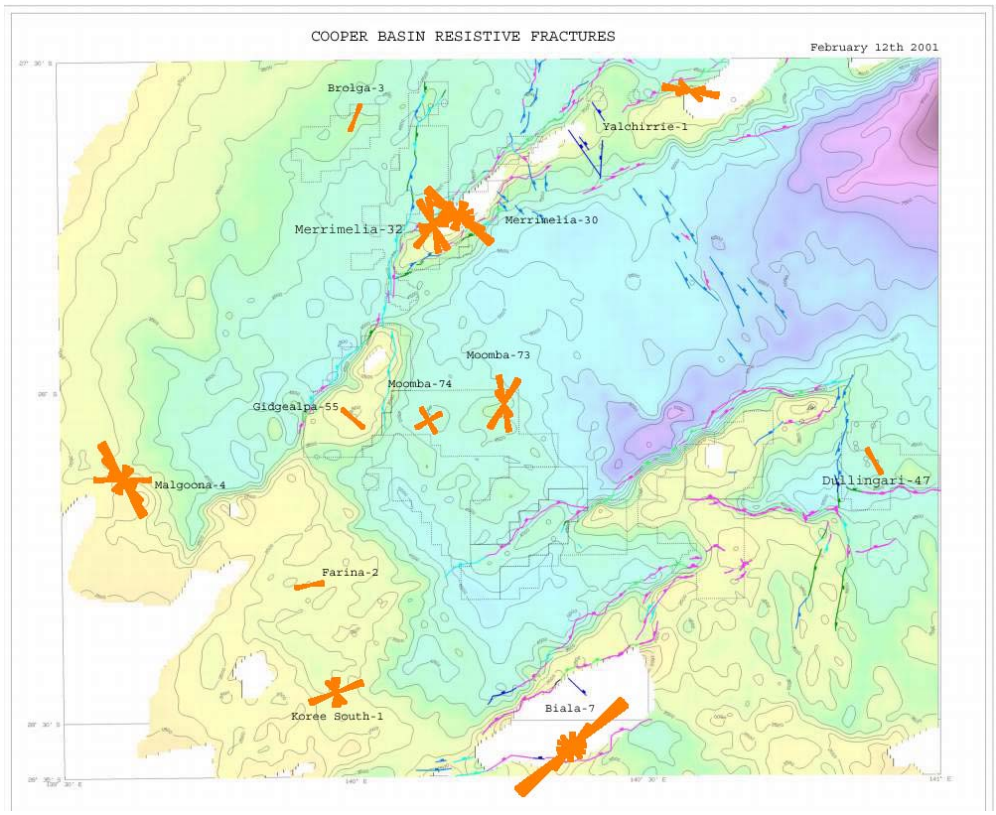

Figure 19 Map of resistive fracture distributions interpreted from resistivity logs in the Cooper basin. Rose petals are length weighted relative to fracture numbers.

Well Name	Log Type	Format	Interpretation Intervals			Number of Fractures		Raw Frac Density	
			Top (ft)	Bottom (ft)	Length (ft)	Conductive	Resistive	Conductive	Resistive
Barina-2	FMS	Digital	6018.28	7079.22	1060.95	11	0	0.010	0.000
Biala-7	FMS	Digital	3368.04	4036.16	668.12	12	13	0.018	0.019
Brolga-3	FMI	Digital	8193.57	9124.01	930.43	5	1	0.005	0.001
Dullingari North-8	FMS	Digital	6499.52	8742.18	2242.66	5	0	0.002	0.000
Dullingari-47	FMS	Digital	4313.01	4823.98	510.97	1	1	0.002	0.002
Farina-2	FMS	Digital	6131.60	7166.55	1034.95	6	1	0.006	0.001
Gidgealpa-55	FMS	Digital	3750.81	3790.43	39.62	4	1	0.020	0.005
Koree South-1	FMS	Digital	5750.69	6891.56	1140.87	8	5	0.007	0.004
Malgoona-4	FMS	Digital	1310.40	6932.43	5622.04	40	14	0.007	0.002
Merrimelia-30	FMS	Digital	5666.99	6967.27	1300.28	60	21	0.046	0.016
Merrimelia-32	FMS	Digital	3901.96	5341.93	1439.97	76	9	0.027	0.003
Moomba-134	CBIL	Digital	10074.00	10491.00	417.00	39	0	0.094	0.000
Moomba-73	FMS	Digital	7571.60	8129.02	557.42	20	6	0.015	0.004
Moomba-74	FMS	Digital	7516.00	7894.00	378.00	15	2	0.036	0.005
Yalchirrie-1	FMS	Digital	6948.68	7914.86	966.19	46	5	0.048	0.005

Table 7 Raw fracture densities calculated by well normalised for image coverage. The data in this table is summarised in Figure 20.

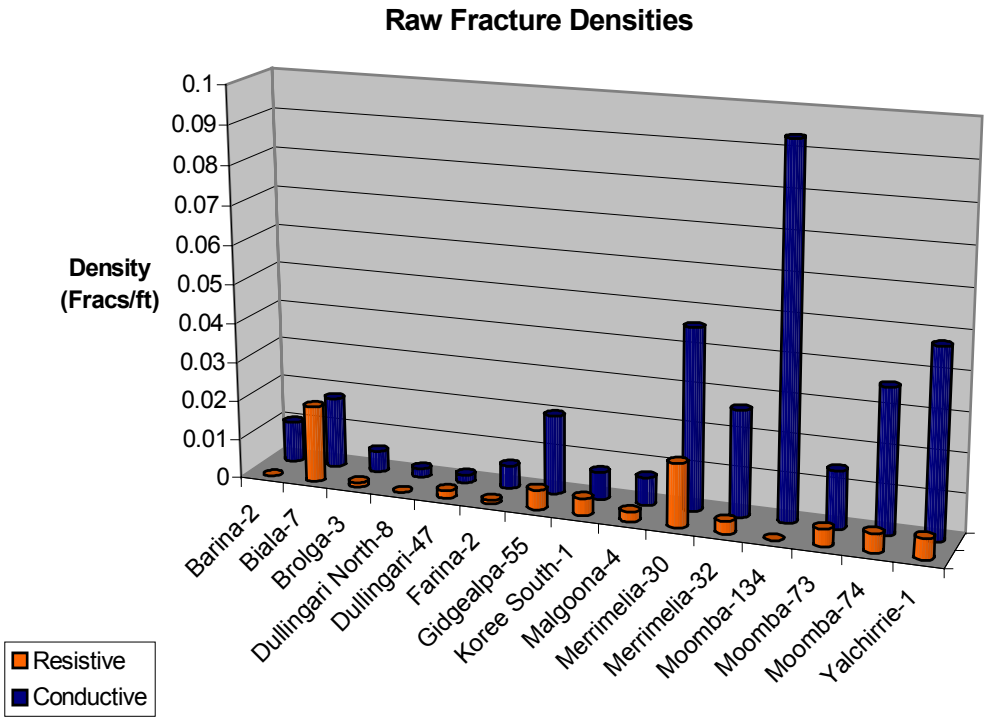

Figure 20 Raw fracture density by well normalised for image coverage.

Formation	Image Coverage (ft)	Number of Fractures		Raw Frac Density	
		Conductive	Resistive	Conductive	Resistive
Bulldog Shale	1019	9	1	0.009	0.001
Wallumbilla Formation	620	44	1	0.071	0.002
Cadna-Owie Formation	621	6	12	0.010	0.019
Murta Member	500	3	0	0.006	0.000
McKinlay Member	120	1	0	0.008	0.000
Namur Sandstone Member	1332	4	4	0.003	0.003
Westbourne Formation	364	3	0	0.008	0.000
Birkhead Formation	144	6	2	0.042	0.014
Basal Birkhead Sand	116	2	0	0.017	0.000
Hutton Sandstone	1578	18	7	0.011	0.004
Poolowanna Formation	426	6	4	0.014	0.009
Nappamerri Group	1132	13	7	0.011	0.006
Toolachee Formation	1668	15	2	0.009	0.001
Daralingie Formation	842	18	0	0.021	0.000
Roseneath Shale	839	1	0	0.001	0.000
Epsilon Formation	694	1	0	0.001	0.000
Murteree Shale	690	4	2	0.006	0.003
Patchawarra Formation	3854	34	2	0.009	0.001
Tirrawarra Conglomerate	132	9	6	0.068	0.045
Tirrawarra Sandstone	76	1	0	0.013	0.000
Merrimelia Formation	451	23	2	0.051	0.004
Pre-Permian	1091	127	27	0.116	0.025

Table 8 Raw fracture densities calculated by formation and normalised for image coverage. The data in this table is summarised in Figure 21.

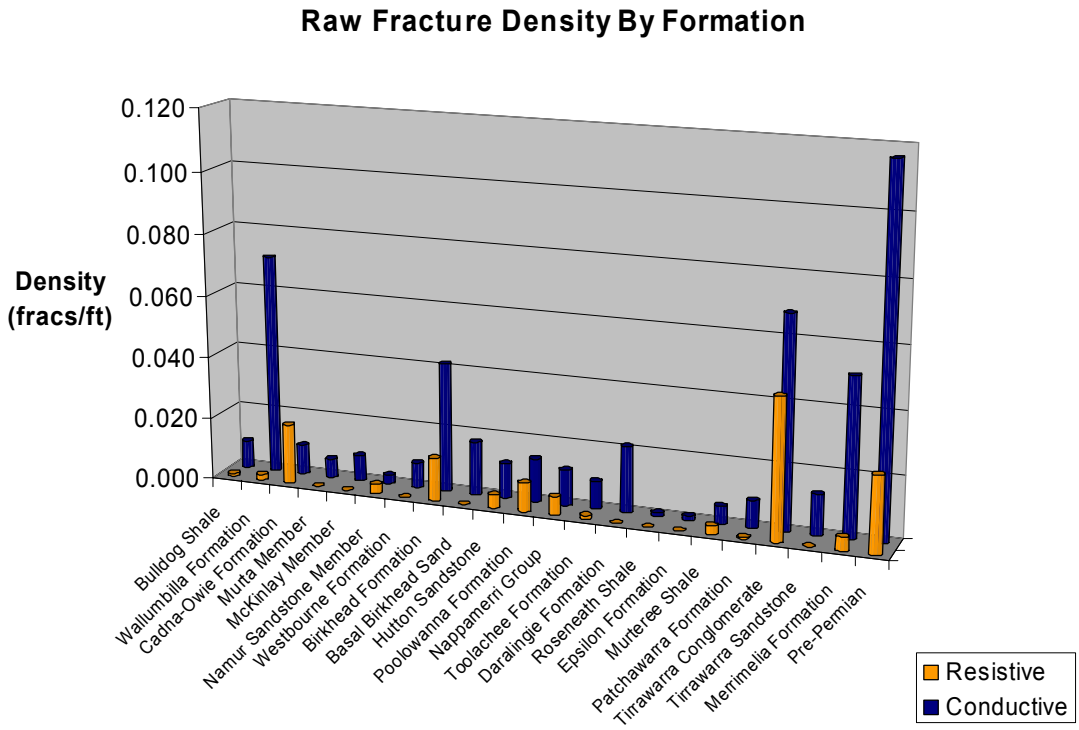

Figure 21 Raw fracture density by formation and normalised for image coverage.

Fracture Susceptibility

Fracture Susceptibility is the key methodology for identifying likely orientations of hydraulically conductive fractures. Given the in situ stress conditions the relative likelihood of fracture reactivation can be assessed in terms of shear and normal failure mechanisms.

All possible fracture orientations lie within the shaded area of a three dimensional Mohr's circle (Figure 22). For a given fracture orientation, the far field stresses can be resolved into shear and normal stress components acting upon that fracture. The susceptibility of that fracture being open within the contemporary stress field can be quantified by the increase in fluid pressure (ΔP) required to cause reactivation i.e. distance from the failure envelope (Figure 22). This is not meant to imply that failure is always due to changes in fluid pressures. Nonetheless, it does provide a simple way of expressing the proximity of a plane of any given orientation to the failure envelope. The ΔP value for each plane is re-plotted on a stereonet of poles to planes (Figure 23). The fracture susceptibility for any pre-existing fracture is then easily read from the stereonet. The advantage of this method is that it considers all modes of brittle failure; extension, shear and extensional-shear.

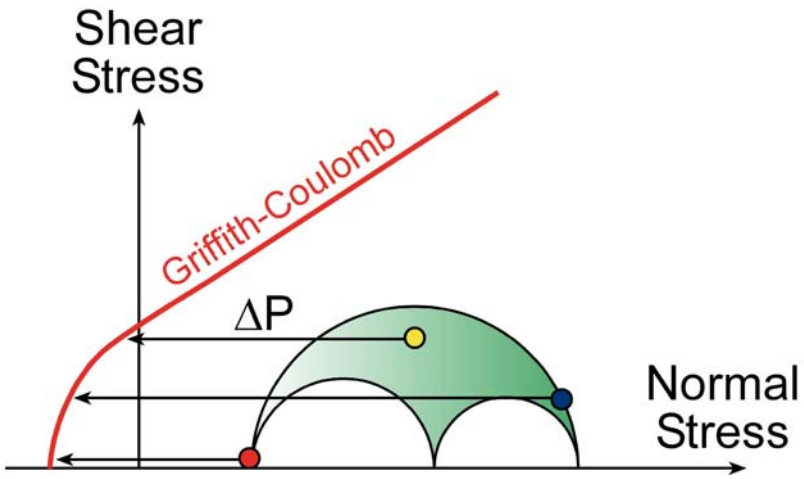

Figure 22 Three-dimensional Mohr diagram with composite Griffith-Coulomb failure envelope. All possible orientations of planes lie within the shaded area. The horizontal distance between any orientation and the failure envelope (which may be thought of as the increase in pore pressure, ΔP, is required to cause failure) is used to assess the susceptibility of a plane to failure.

Fracture susceptibility stereonets have been produced for several regions of the Cooper Basin based on the stress tensor data presented in the previous chapter. These stereonets have been superimposed on a horizon map of the basin to illustrate the change in susceptibility of fracture orientations Figure 24. The in situ stress tensor is on the boundary of a strike-slip and thrust regime. Hence there is little difference in magnitude between σ_{hmin} and σ_v. These conditions dictate a large proportion of fracture orientations to have high fracture susceptibility (Figure 25).

This fracture susceptibilitydistribution is very similar in stereonets calculated for the changing stress field across the Cooper Basin. Each shows high fracture susceptibilities for a wide range of fracture orientations. In general, fractures dipping > 60° and striking NW-SE or ENE-WSW have the greatest fracture susceptibility and sub-vertical fractures striking N-S have the least fracture susceptibility.

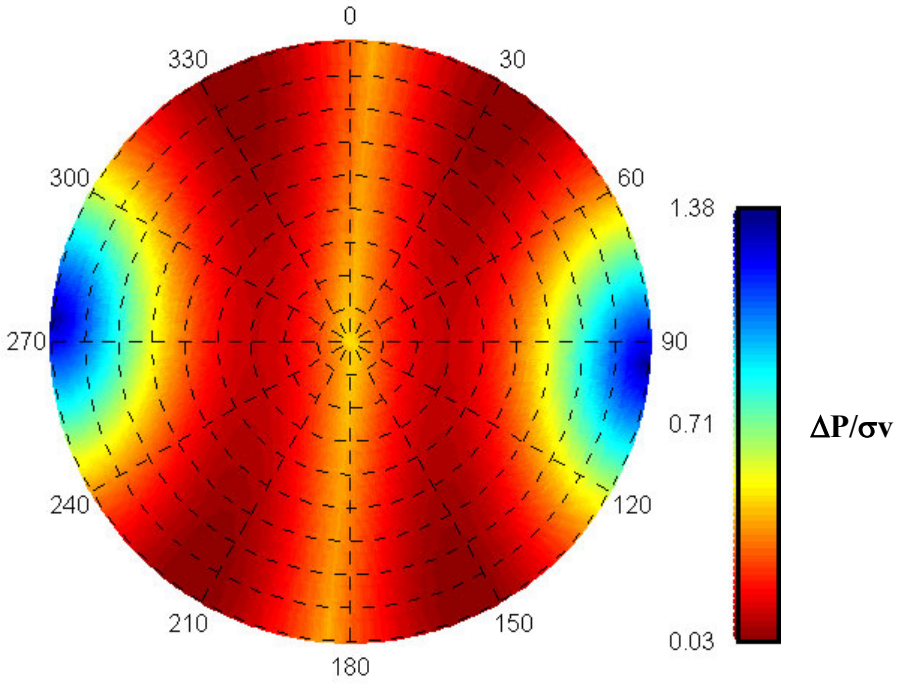

Figure 23 Example fracture susceptibility stereonet calculated for relative stress magnitudes in Moomba-73. All fracture orientations are plotted as poles to planes on a southern hemisphere, equal angle projection. Scale is normalised relative to σv. Red indicates fracture orientations with greatest susceptibility for reactivation i.e. likely to be open and hydraulically conductive. Blue indicates fracture orientations with least susceptibility for reactivation.

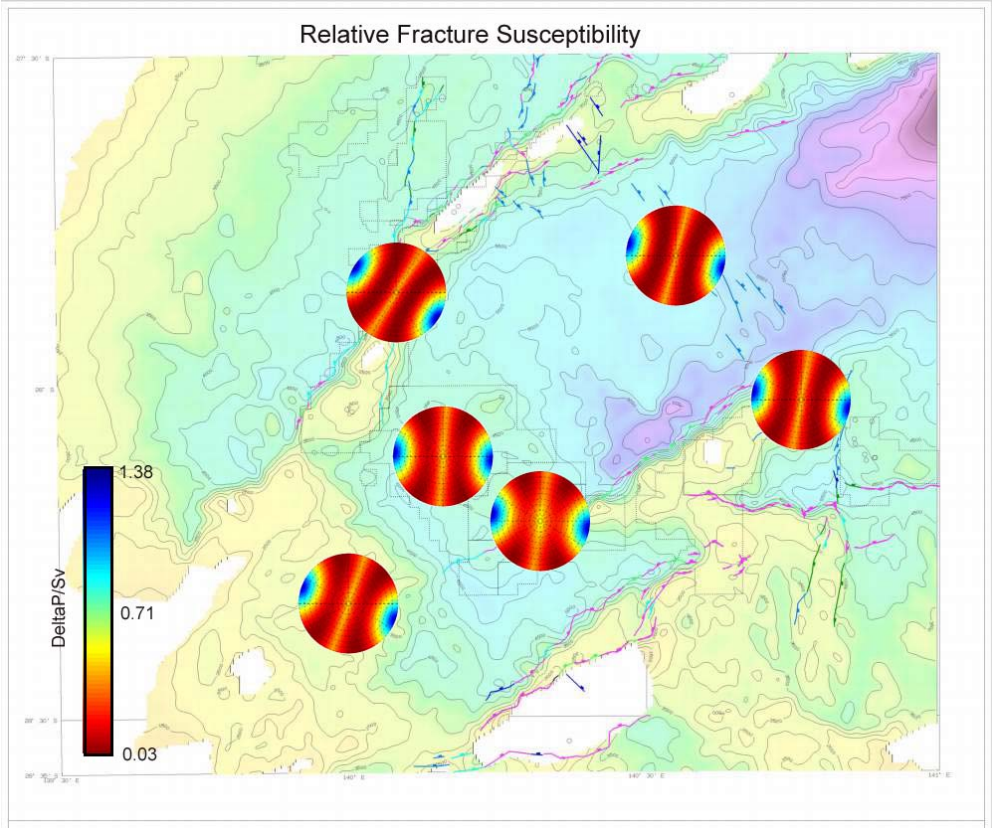

Figure 24 Comparison of fracture susceptibility stereonets across the Cooper Basin.

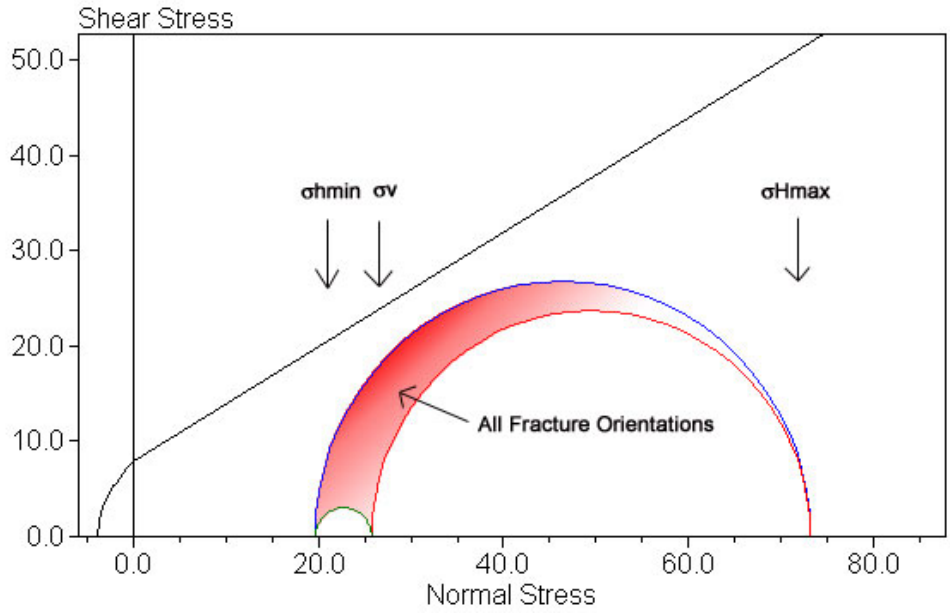

Figure 25 3D Mohr diagram of stress conditions at Moomba-73 illustrating that a large proportion of fracture orientations have a high fracture susceptibility i.e. relatively close to failure.

Conductive natural fractures are commonly interpreted as open and hydraulically conductive when interpreted from borehole images. Conversely, resistive fractures are viewed as cement filled fractures that are not hydraulically conductive. A comparison of observed conductive fracture orientations with a corresponding fracture susceptibility prediction can calibrate the methodology as a predictive tool.

In the Cooper Basin this comparison suggests that the majority of conductive fractures are associated with high fracture susceptibility orientations (Figure 26). The orientations of highest susceptibility correspond to the dominant conductive fracture orientations. Therefore, given a genetic model of fracture origin, fracture susceptibility can predict which pre-existing fractures are open and hydraulically conductive in the Cooper Basin.

Factors that will enhance the likelihood of hydraulically conductive pre-existing fractures corresponding with predicted high susceptibility orientations are increased pore pressure and greater differential stress. An increase in pore pressure corresponds with a decrease in effective stress putting the environment closer to failure (3D Mohr circle moves towards the failure envelope i.e. to the left). A greater differential stress ($\sigma1$-$\sigma3$) also increases likelihood of failure (diameter of the Mohr circle increases towards failure envelope).

Mudweight was mapped as a proxy for pore pressure in Chapter 3 (Figure 4, Figure 5 and Figure 6). The greatest pore pressures occur within the Nappamerri Trough and increase with depth. Differential stress is shown for the Toolachee and Patchawarra Formations in Figure 27 and Figure 28. These figures indicate that there is an increase in differential stress along the axis of the Nappamerri Trough in a northeast direction and also in a northerly direction. Differential stress also increases with depth.

This evidence, in conjunction with the observation that the greatest fracture densities occur in Pre-Permian Basement, suggests that the greatest potential for exploiting hydraulically conductive natural fractures is at depth in the Nappamerri Trough, possibly towards the northern margin, in the sediments of the Warburton Basin.

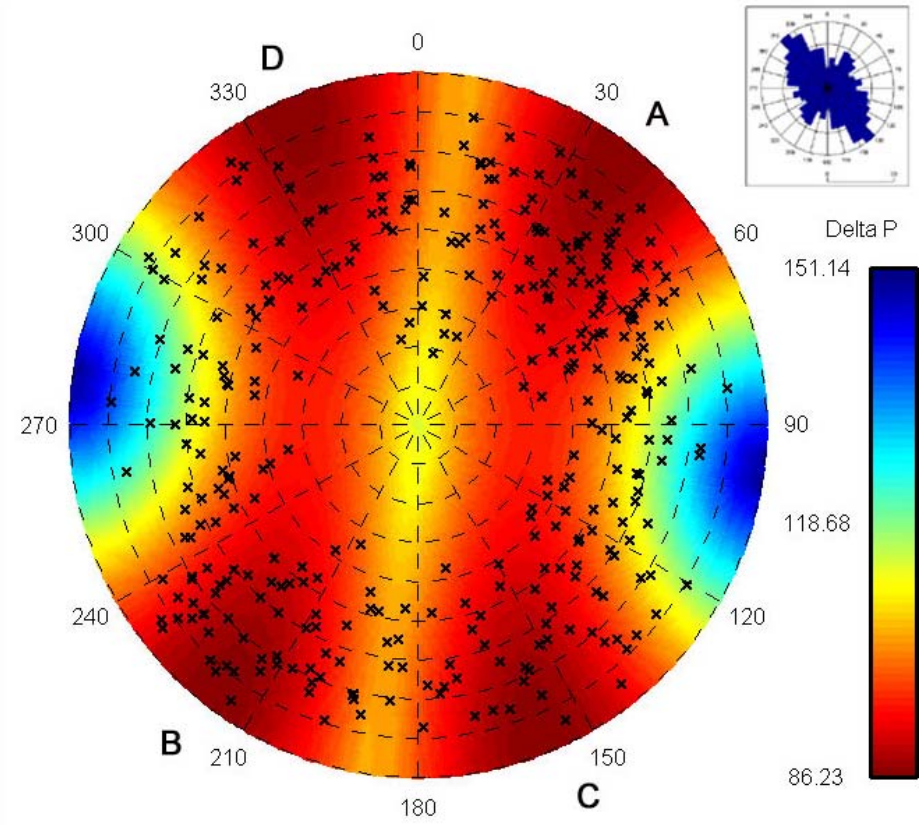

Figure 26 Comparison of fracture susceptibility (calculation using Moomba stress tensor) and observed conductive fracture orienatations from image logs. Highest susceptibility regions at points A and B correspond with the dominant conductive fracture strike direction (inset). Similarly, high susceptibility points C and D correspond with secondary strike oriented NE-SW.

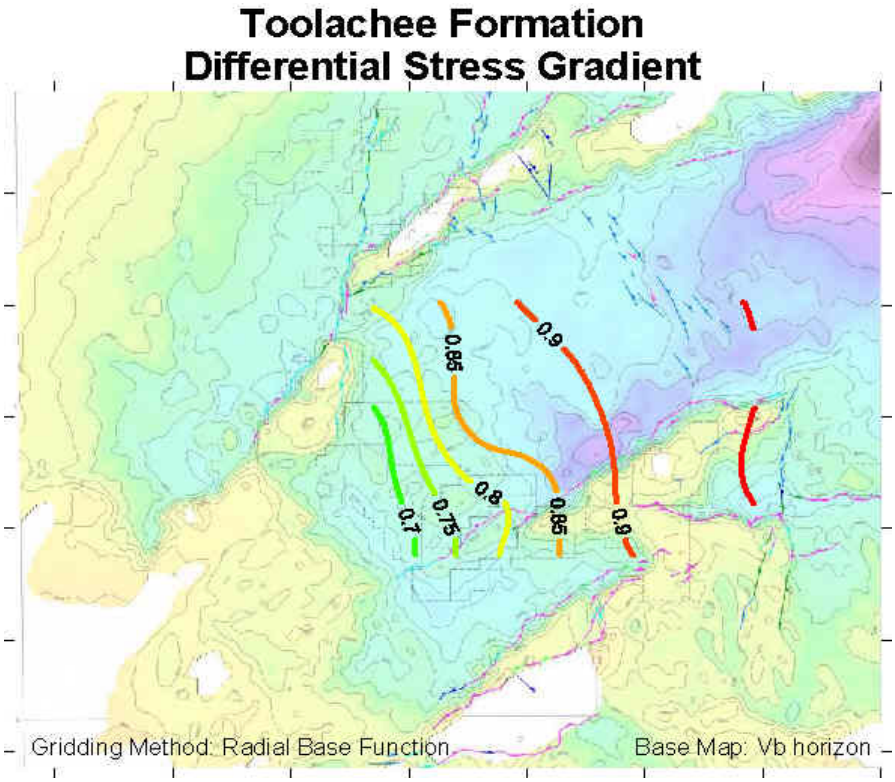

Figure 27 Toolachee Formation differential stress gradient ($\sigma_{Hmax} - \sigma_{hmin}$) in psi/ft.

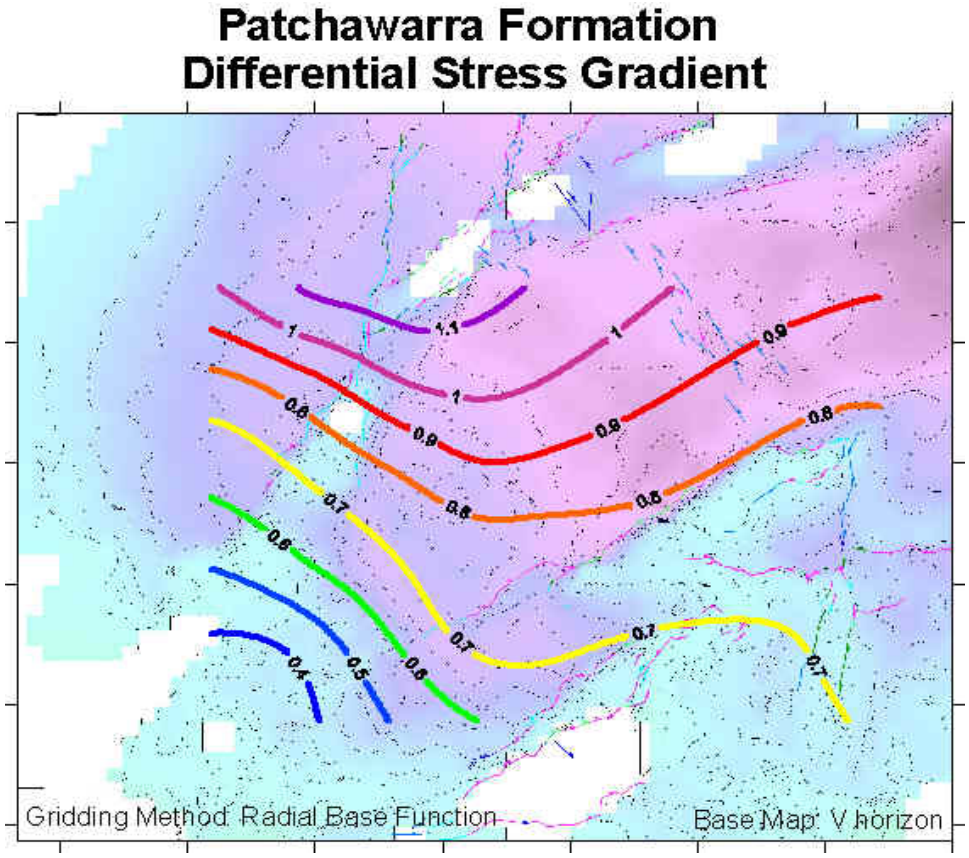

Figure 28 Patchawarra Formation differential stress gradient ($\sigma_{Hmax} - \sigma_{hmin}$) in psi/ft.

5. Overpressure Analysis

Pore pressure analysis is an important aspect of the stress tensor. The occurrence of non-hydrostatic pore pressures influences the distribution of open natural fractures. The pore pressure part of the project focuses on compiling observed pore pressure data (mud weights, drill stem tests, and wireline formation interval tests), and inferring pore pressures from wireline logs.

Observed Pressure Data

Pressure information from formation tests and mudweights was compiled and has been include in the results database (See Chapter 7). The observed pressure data included in the database contains:

- 85 wells included in pore pressure study;
- mud weight measurements from 62 wells;
- RFT measurements from 20 wells, and;
- DST measurements from 78 wells.

On the basis of this information the following statements can be made. The normal or hydrostatic gradient in the Cooper Basin is 0.455 psi/ft. Significant overpressure in the Cooper Basin has only been observed in the Burley, McLeod, Kirby and Bulyeroo structures in the deep, hot Nappamerri Trough. Overpressured DST extrapolated pressure measurements are found in three wells, Burley-1, Kirby-1 and McLeod-1. There are three extrapolated DST pressure measurements in Kirby-1 (Figure 29). DST no. 4 (Toolachee) which is normally pressured, DST no. 8 (Patchawarra) that is overpressured and DST no. 9 (Patchawarra) which is also overpressured. There is also an overpressured DST shut in pressure in DST no. 12 (Lower Patchawarra?). The maximum pressure gradient encountered in Kirby-1 was 0.730 psi/ft (DST no. 12). The magnitude of the excess pore pressure in the three overpressured DSTs increases with depth. The rate of increase is steeper than the hydrostatic gradient. Hence the following statements can be made:

- The sequence between the overpressured DST measurements is not in hydraulic communication and thus must be compartmentalised;
- The origin of overpressure is not related to hydrocarbon buoyancy unless each of the overpressured compartments has large down dip hydrocarbon columns, and;
- The sequence between the overpressured DST measurements is a pressure transition zone.

In addition to the Napamerri Trough wells there is also slight overpressure in the Moomba North area, Moomba-55 DST no. 5 had a pressure gradient of 0.557 psi/ft.

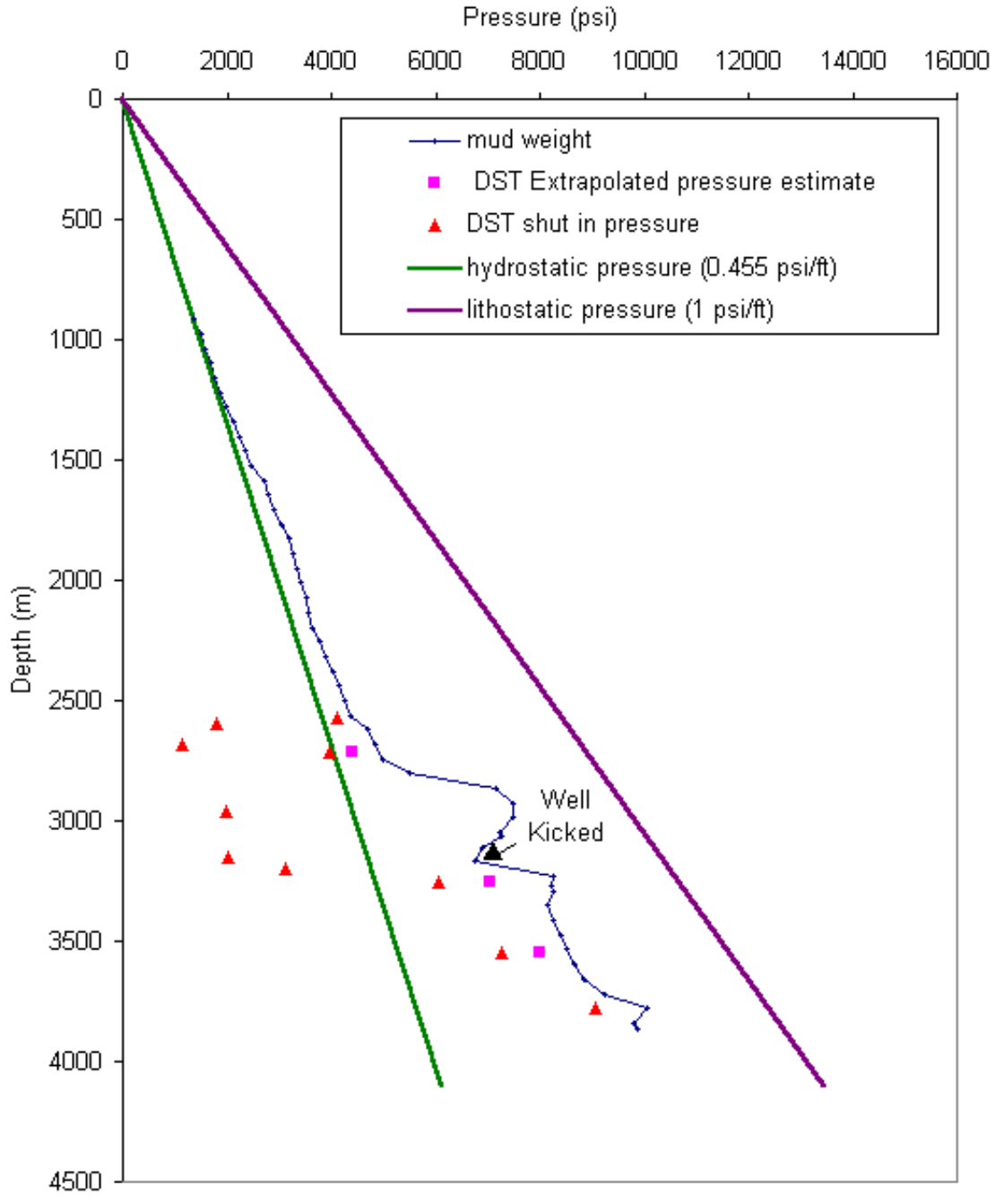

Figure 29 Kirby 1 pressure versus depth.

Due to the lack of direct pressure measurements in the overpressured sediments the top of overpressure is hard to pick. However, the top of the overpressure in Kirby-1 is between DST no. 4 and DST no. 8 (2717-3257 m). The lateral extent of the overpressure away from the central Nappamerri Trough wells could not be determined from this study. Similarly the lateral seals to the pressure compartments, which must exist, could not be delineated from the available data. No model for the lateral sealing of the pressure compartments is suggested here. Knowledge of the origin of the overpressure is vital for any attempt to model overpressure away from well control.

Wireline Log Analysis

Wireline log analysis was performed on a sub-set of wells in order to infer pore pressure (Table 9).

Well	Observed Data	Eaton Method	Inferred Relative Uplift Using Sonic Log (m)
Big Lake 27	normally pressured	normally pressured	
Bulyeroo 1*	overpressured (MW)	overpressured	100
Burley 2	overpressured (MW)	overpressured	200
Darmody 1	normally pressured	normally pressured	100
Kirby 1	overpressured (DPM)	overpressured	200
McLeod 1	overpressured (DPM)	overpressured	200
Moomba 55	mildly overpressured	overpressured	150
Moomba 78	normally pressured	normally pressured	
Snake Hole 1	normally pressured	normally pressured	0
Strathmount 1	normally pressured	normally pressured	
Swan Lake 1	normally pressured	normally pressured	
Swan Lake 4	normally pressured	normally pressured	
Three Queens 1	normally pressured	normally pressured	250
Wantana 1	normally pressured	normally pressured	100
Wantana 2	normally pressured	normally pressured	

Table 9 Wells included in wireline log analysis. Apparent relative uplift estimates are also shown where available. Uplift estimates are not absolute as they only refer to relative uplift between the wells analysed in this study. Inferred relative uplift is the amount of uplift compared to Snake Hole 1, which had the largest positive correction applied to the normal compaction trend.

Sonic normal compaction trend and uplift determination

A sonic normal compaction trend was established by fitting an exponential trend line to edited sonic log values (Figure 30). This trend is based on the Athy (1930) equation. The sonic normal compaction trend obtained for the Cooper Basin is:

$$\Delta t = 200 + 455 \exp^{(-0.001(z+UC))}$$

where UC is the uplift correction, Δt is the sonic log acoustic travel time and z is depth.

The application of a regionally derived normal compaction trend to individual wells in the Cooper Basin was complicated by uplift. The effect of uplift was removed by fitting the normal compaction trend to the upper, assumed normally pressured, sections in each well (above Top Toolachee). The relative uplift was then measured by the amount of adjustment applied to the normal compaction trend (Table 9).

Eaton (1972) Pressure analysis

As part of the wireline log analysis the Eaton quantitative pressure method was applied the to the sonic log in 15 wells. The pressure profile from Strathmount-1 is shown as an example of this technique in Figure 31. Pressure estimates resulting from the wireline log analysis are included in the Results Database (Chapter 7). A more detailed account of the Eaton (1972) pressure analysis is given in van Ruth and Hillis (2000). A digital version of this paper is also included in the Results Database.

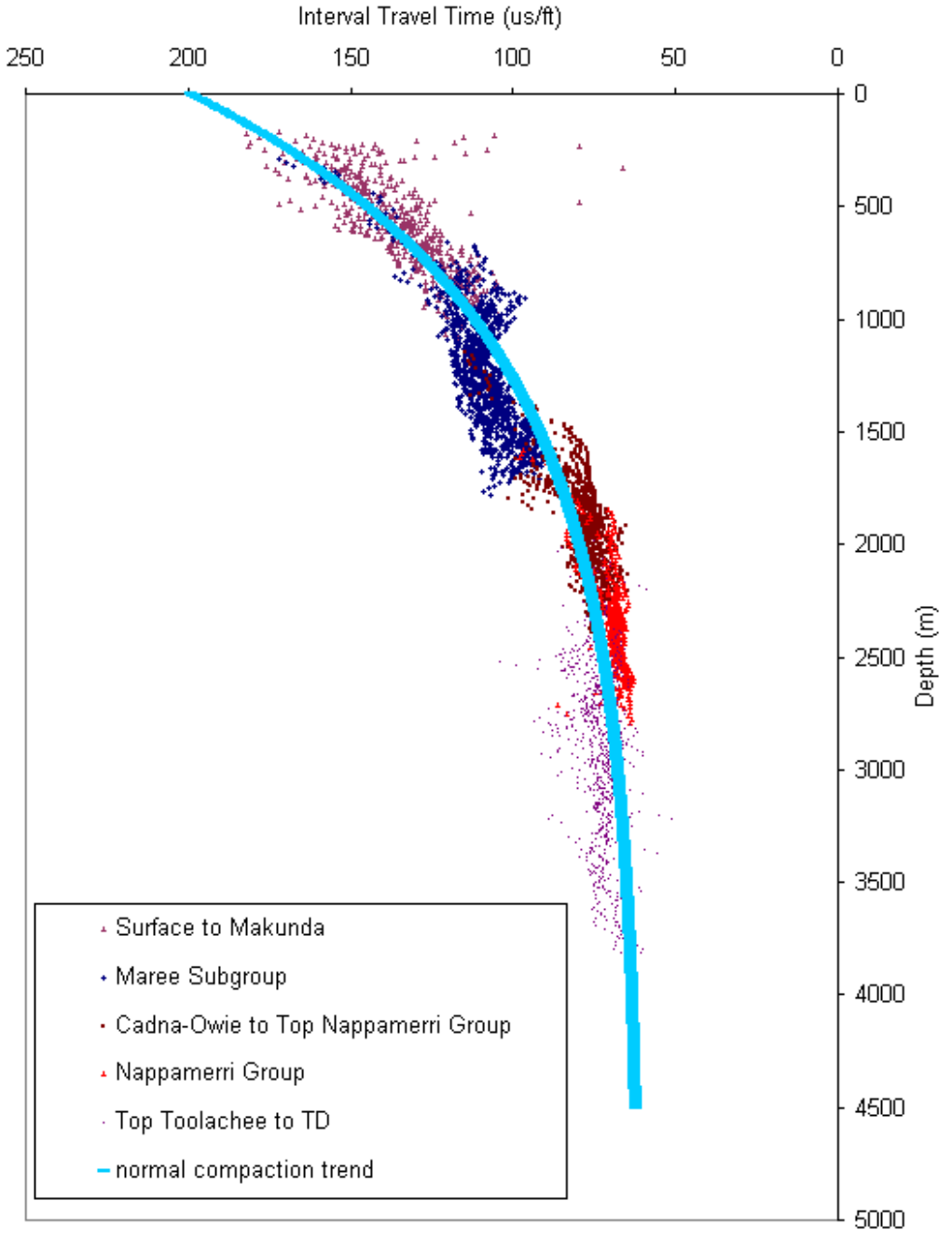

Figure 30 Sonic log derived normal compaction trend based on the Athy (1930) equation.

Velocity effect of Overpressure – implications for seismic detection

The size of the velocity anomaly associated with the overpressured sediments in the Nappamerri Trough is approximately 35 us/m as seen on the fully edited sonic log in Figure 32. The partially edited sonic log was smoothed, despiked and edited for coal seams using a sonic log cut-off. All the editing could be applied to seismic velocity data and thus the partially edited sonic log is a better gauge of what could be determined from seismic velocity data. The partially edited sonic log also displays the 35 us/m anomaly. Hence, the seismic resolution that is required for detecting the velocity anomaly associated with the overpressure in the Nappamerri Trough is approximately 35 us/m.

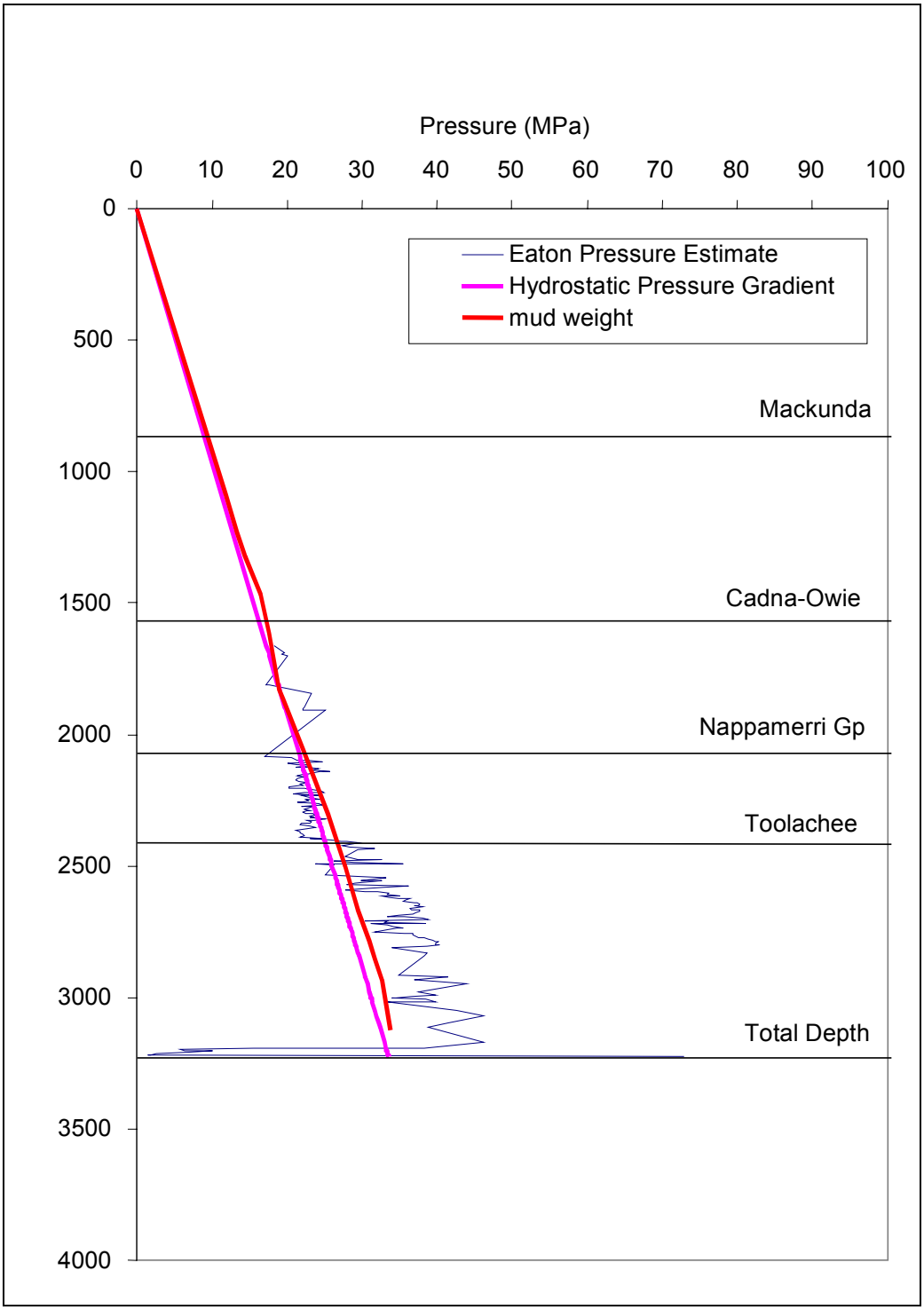

Figure 31 Strathmount-1 Eaton Pressure versus depth. Mud weight, and hydrostatic gradient have also been plotted.

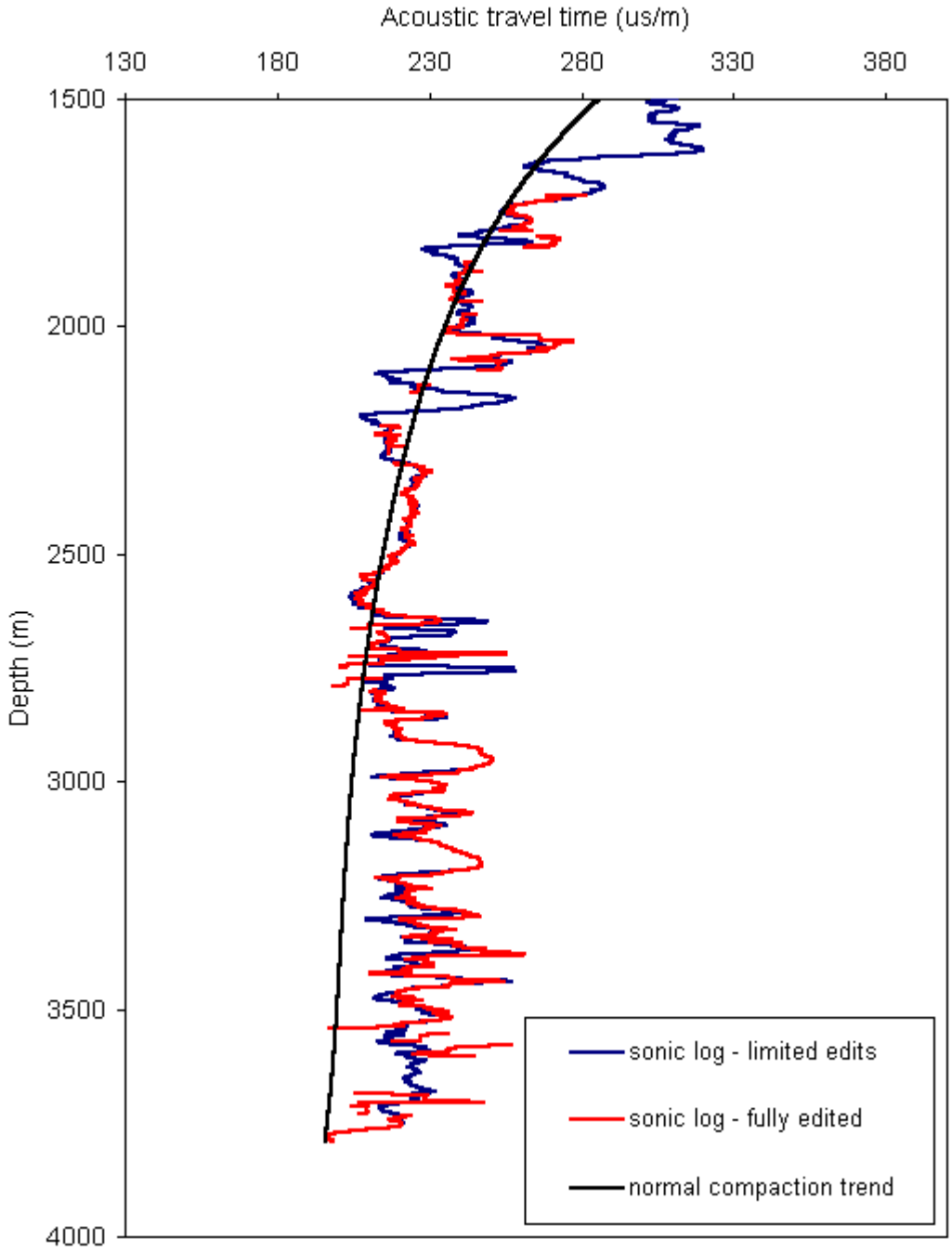

Figure 32 McLeod-1 acoustic travel time versus depth for the normal compaction trend, the fully edited sonic log and the partially edited sonic log. Editing was limited to what could be applied to the sonic log in isolation.

6. Stress Modeling Pilot Study

Introduction

The numerical technique known as stress mapping is used as a way of predicting the perturbation of stress (orientation and magnitude), resulting from the influence of complex rock and fracture geometry on the regional stress state. Two and three dimensional models have been used previously for structural targeting in mineral exploration. The method predicts zones of low minimum stress indicating potential for pore fluid accumulation and hence epigenetic mineral deposition (Mair et al, 2000). This method is also applicable to the oil industry where stress perturbations caused by geological heterogeneity can give rise to zones of enhanced oil accumulation. This could prove to be a key exploration technique in the case of unconventional deep basin gas deposits. For these deposits commercial exploitation lies not in intersecting gas but rather in intersecting zones of enhanced porosity and permeability in generally tight sandstones, typical of deep basin settings (Hillis et al, 2001). Zones of low minimum stress are expected to be coincident with high porosity/permeability.

Su and Stephansson (1999) studied the effect of a single fault and fault parameter sensitivity, on the orientation and magnitude of in-situ stress under the action of a regional stress field by numerical modeling using the two-dimensional distinct element method and the code UDEC (ITASCA). They found that the range of stress variation is strongly determined by the friction angle (φ). A pilot study was carried out in the Big Lake region in the Cooper Basin, South Australia and a comparison was made with instantaneous shut-in pressure (ISIP) data, for the minimum horizontal stress magnitude, previously obtained for that area. The Big Lake fault geometry example, demonstrated a high sensitivity to fault friction angle and the resultant stress concentrations, as suggested by Su and Stephansson (1999).

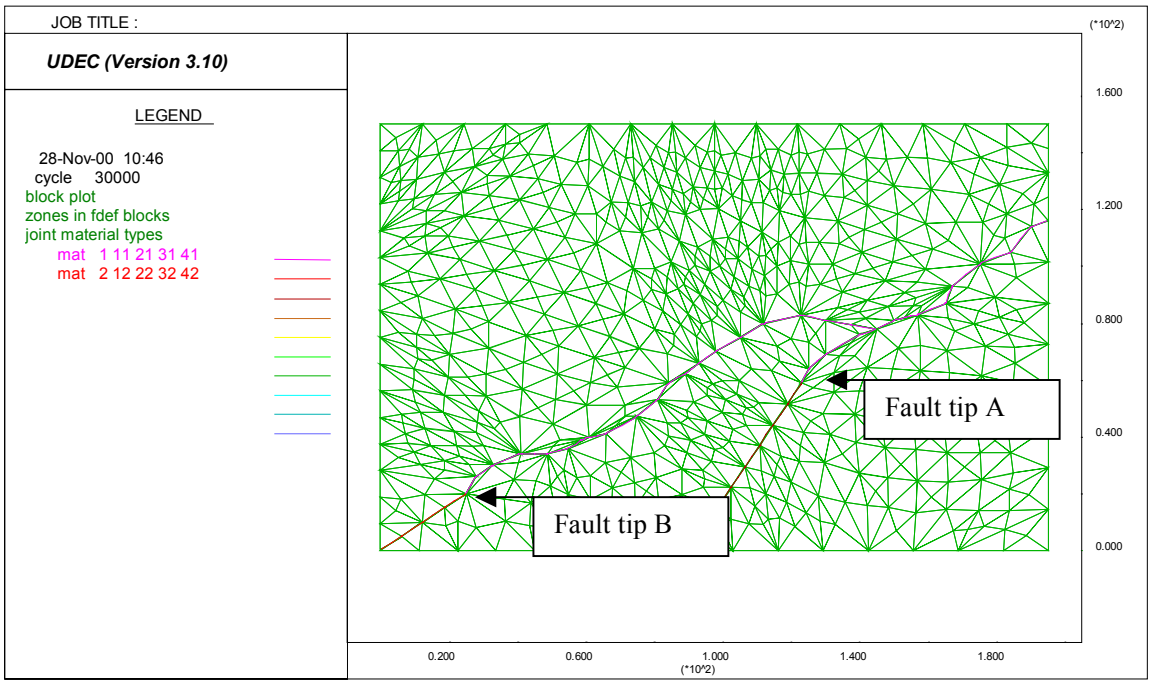

Figure 33 Fault geometry and block finite difference grid. Mat 1 =actual faults, mat 2 = fictitious faults. Fault tip A and B show junction between fictitious and actual faults.

Geometry of Example Model

The geometry of the model is given in Figure 33, a single NE-SW trending faults, splits into two faults, fault A (eastern) and fault B (western). The model used the elastic and isotropic model for intact rock and Mohr-Coulomb model of fracture strength. Both faults are non-persistent and do not extend to the model boundary, in order to do this fictitious fault parameters are used as described by Su and Stephansson (1999). The model was run using a constant in-situ regional stress ratio of $\sigma_{hmin}<\sigma_v<\sigma_{Hmax}$=4:5:12. The intact rock properties and fictitious faults properties were held constant and a sensitivity study was carried out by varying fault normal stiffness, fault shear stiffness, and fault friction angle.

Sensitivity to model parameters and interpretation of stress mapping results

The results (Figure 34) showed a stress low between the two faults, located opposite fault tip A on the eastern side of fault B, this compared well with ISIP (instantaneous shut-in pressure) results obtained from boreholes. ISIP results for the minimum horizontal stress were plotted as contours (Geomechanics Int. Big Lake Report), showing a decrease in stress from 1.1 psi/ft to 0.8psi/ft. This region was located within the fault bound region to a location opposite fault tip A, as shown in the modeling results. The modeling results also clearly demonstrated a stress drop from 59.8MPa to 43.3MPa or 8,800psi to 6,365psi over 9,000ft giving 0.97psi/ft to 0.71psi/ft. This stress drop compares well with the ISIP data.

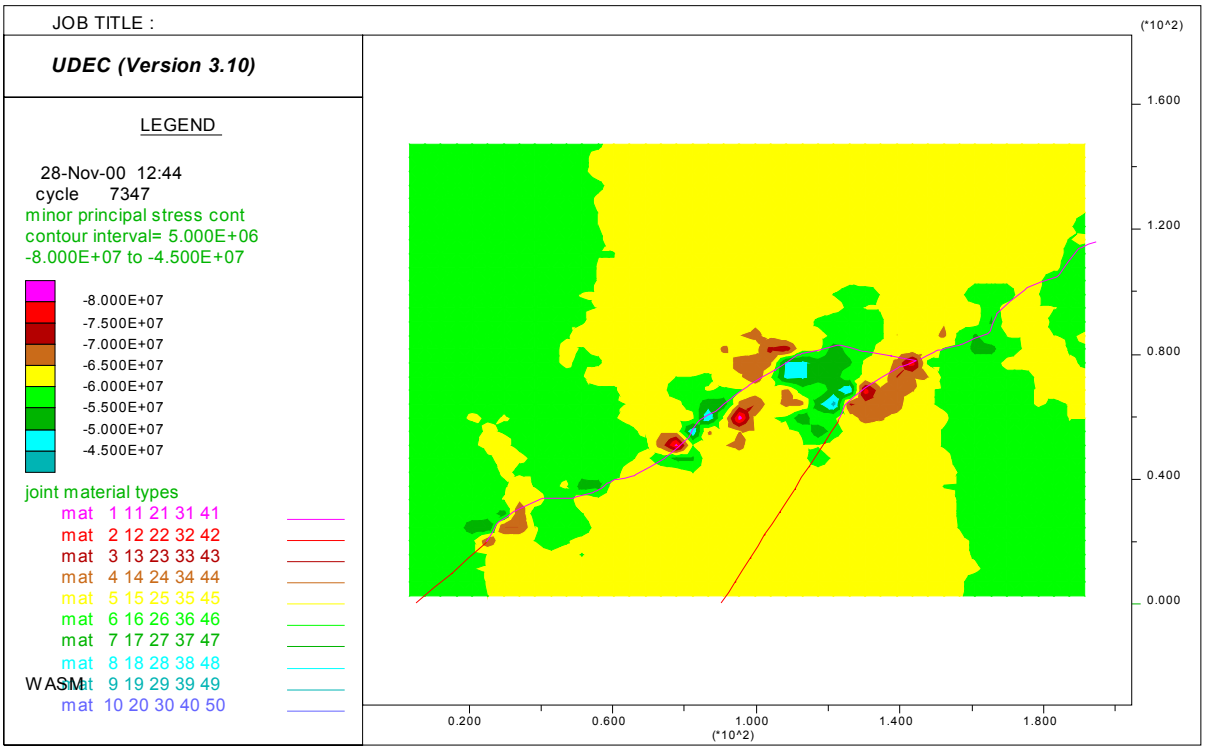

Figure 34 Shaded contour map showing minimum horizontal stress magnitudes (negative values represent compression).

Perturbation of the stress orientation was also studied. The principal stress vectors were plotted in the zones of the deformable blocks. It was observed that the stress vectors showed slight tilting of σ_H maximum and σ_h minimum, of approximately 5-20° from NS/EW to NNE/SSW, this was also in agreement with the borehole breakout orientation data.

The magnitude variation of the low decreased as the joint stiffness was increased. The exact location of this low varied slightly according to the fault friction angle, interestingly a critical value for the friction angle was observed, at less than 30° fault B was activated and right lateral displacement was observed across the faults. At greater than 30°, the majority of NE-SW trending portion of fault B was not activated, but the E-W trending portion showed left lateral displacement. This effect produced a slight re-positioning of the stress low.

Further maps were included in the pilot study, the Central Nappamerri Trough and a large scale map of the Nappamerri Trough region. Regions of stress minima were found but other stress data is limited in this region so no comparison has yet been made.

Summary

The results of this study demonstrate the UDEC model can be used to predict locations of stress minima. For the geometry under investigation the exact location of the predicted stress low is highly sensitive to fault friction angle, and the magnitude of the stress low is affected by fault stiffness parameters.

7. Results Database

The results database is a Microsoft Access repository for all interpretation data and information pertaining to the ARC SPIRT Project year 2. Although not originally specified as a project deliverable, the database will dramatically aid technology transfer at the conclusion of the project. Other advantages of the database include:

- one repository for all analyses related to the project including stress data, fracture types, resistivity images, reports and basic well information;
- easily accessible results that can be exported in table format (Excel or similar);
- integrated with stratigraphy (lithostratigraphic and chronostratigraphic) in order to assess results by horizon, and;
- powerful data retrieval.

A CD containing the Results Database is included as Enclosure 2.

8. References

Athy, L.F., 1930. Introduction to Petrophysics of reservoir rocks, *AAPG Bull.*, 34, 943-961.

Eaton, B.A., 1972. Graphical method predicts geopressures worldwide: World Oil, 182, 51-56.

Greenstreet, C.W., 1999. Vertical stress characterization Big Lake in situ stress study, Santos Memorandum GR99-439, 15p.

Hillis, R.R, 1996. FMS Log Image Interpretation and the Contemporary Stress Field of the Nappamerri Trough: Implications for Fracture Stimulation of Tight Gas Prospects and the Stability of Horizontal Wellbores, Santos Report, p37.

Hillis, R.R., Morton, J.G.G., Warner, D.S and Penney R.K. Deep Basin gas: A New Exploration Paradigm in the Nappamerri Trough, Cooper Basin, South Australia. Appea Journal, 2001.

McGarr, A. & Gay, N.C., 1978. State of stress in the Earth's crust, *Ann. Rev. Earth Planet. Sci.*, 6, 405-436.

Mair, J.L., Ojala, V.J., Salier, B.P., Groves, D.I. & Brown, S.M.(2000) *Application of stress mappping in cross-section to understanding ore geometry, predicting ore zones and development of drilling strategies*. Australian Journal of Earth Sciences. 47, 895-912.

Su, S. and Stephansson. 1999. *Effect of a fault on in situ stresses studied by the distinct element method*. International Journal of Rock Mechanics and Mining Sciences. 36, 1051-156

van Ruth, P. & Hillis, R.R., 2000. Estimating pore pressure in the Cooper Basin, South Australia: sonic log method in an uplifted basin, *Exploration Geophysics*, 31 441-447.

ARC SPIRT Project

EXPLORATION FOR TIGHT GAS RESERVOIRS ENHANCED BY NATURAL FRACTURING, COOPER BASIN, SOUTH AUSTRALIA

Collaborators:

Santos Ltd
LDG Task Force

And

NCPGG
University of Adelaide

Six Month Progress Report
(27th August 2000)

Executive Summary

This ARC SPIRT project aims to identify where natural fractures enhance reservoir permeability in the 'tight' gas reservoirs of the Nappamerri Trough. The current phase of the project focuses on natural fracture "sweet spot" prediction with respect to the in situ stress field. In situ stress analyses to date suggest:

- the Cooper Basin Stress Map illustrates a consistent ≈ 100ºN σ_{Hmax} orientation in the Nappamerri Trough;
- three wells north of the GMI structural trend have average σ_{Hmax} orientations ≈ 140ºN (Brolga-3, Moorari-7 and Woolkina-1);
- three wells south west of the Moomba Field have average σ_{Hmax} orientations ≈ 130ºN (Farina-2, Koree South-1 and Daralingie-10);
- no unequivocal stress rotations associated with faults have been observed;
- Moomba minifrac data suggest pore pressure reduction due to field depletion causes an associated reduction in minimum horizontal stress magnitude;
- depletion must be considered to successfully predict stress distribution and hence fracture 'sweet spots';
- fracture susceptibility prediction suggests the most likely orientation for open fractures with respect to the far-field stresses in the Moomba Province are those striking 060-140ºN and dipping greater than 60º to the north or south;
- the optimal drilling trajectory for fracture intersection in the Moomba Province is a borehole deviated 60-90º towards 150-230ºN or 330-050ºN;
- 223 conductive fractures, 63 resistive fractures, 153 breakout-related fractures and 20 faults were interpreted from 12 FMS/FMI image logs;
- a population of drilling induced conductive fractures (of both shear and tensile types) may exist and must be distinguished from natural fractures because they would not be expected to be open away from the wellbore;
- initial selection of wells for pore pressure analysis has been made and the Eaton quantitative pressure method has been performed on Swan Lake-1, Wantana-1 and Strathmount-1;
- a Microsoft Access "Result Database" is under development to provide a single resource for all project analyses and related information.

Status of Deliverables For End of Year 2 (2000)

AS OF 12th JULY 2000

DELIVERABLE	STATUS AS OF 12th JULY 2000
Technology Transfer of Regional Structural History Phase of Project (a) Report on structural history of Cooper Basin (b) Report on trishear modeling methodology (c) Hillis and/or Flottmann presentation at LDG Forum (circa March 2000) if requested	In communication with Flottman to integrate core analyses into current project phase result database Trishear modeling report completed LDG Forum presentation not required
Regional In Situ Stress Overview: Compile all Existing Data and Analyse Any as Yet Unanalysed Data (eg. FMS logs) (a) Horizontal stress orientation (analysis of all processed FMS logs) (b) Vertical stress magnitude (regional checkshot velocity compilation, and density log integration for at least 10 wells in excess of those done by Santos) (c) LOP and minifracture analysis (all available) for minimum horizontal stress (d) Maximum horizontal stress bounds	Compilation of pre-existing stress interpretations (20 wells) completed. Analysis of newly acquired data: 12 image logs (FMS/FMI) and 5 paper caliper logs (SHDT) No additional vertical stress magnitude calculations as yet LOP, Minifrac and Maximum horizontal stress bounds analyses performed as required (Stress tensor for Three Queens and Moomba areas completed) Additional fracture analyses performed on image log interpretations
Overpressure Analysis (a) Compilation of formation tests, mud weights etc. to delineate observed data on overpressure (b) Analysis of log, especially velocity signature of overpressure (c) Determination of velocity effect of overpressure and input on likelihood of its detection using seismic velocities (d) Determination of the likely lateral and vertical extent of the overpressure	Initial well selection process for pore pressure database Eaton pressure estimates for Strathmount-1, Swan Lake-1 and Wantana-1
In Situ Stress Prediction (a) 2D regional models of effect of discontinuities on in situ stress field with calibration against observed data: eg. possibility of low stress zones in the viscinity of faults (b) Relationships predicting stress in the deep Nappamerri Trough combining depth, overpressure and other relevant parameters (calibrated by observed data) (c) Models and/or observational data on pore pressure, temperature/stress coupling.	An alliance between the NCPGG group undertaking the SPIRT project and Tony Meyers of the University of South Australia has been formed to create regional 2D models of in situ stress distribution around discontinuities. The relationship between reservoir pressure and minifrac closure pressure has been assessed within the Moomba Province.
Reporting (a) Formal progress reports at six-monthly intervals (b) Project management meetings on a quarterly basis	First six-monthly status report presented herein Project management meetings held on 24/3/2000 and 12/7/2000

Introduction

This project aims to identify where natural fractures enhance reservoir permeability in the 'tight' gas reservoirs of the Nappamerri Trough. The first phase of this project (1999) identified key events in the tectonic history of the Cooper Basin that may have contributed to the formation of natural fractures through time. The current focus of the project (2000) is to predict the vertical and aerial distribution of stress in the Nappamerri Trough and the contribution of pore pressure and temperature to the in situ stress state of the target reservoirs. These data can then be integrated to highlight natural fracture plays or 'sweet spots' that can be exploited for hydrocarbons.

Work for this phase of the project has concentrated on the following areas:

1. Stress Orientations
2. Stress Tensor
3. Fracture analysis
4. Overpressure Analysis
5. Results Database

This report will briefly address the progress in each of these areas and plans for the remainder of the year. The work reported here was conducted by Scott Mildren (NCPGG Postdoc, University of Adelaide) and Peter Van Ruth (NCPGG PhD Student, University of Adelaide) in close consultation with David Warner (Senior Staff Geologist, Santos LDG Task Force) and Richard Hillis (NCPGG, University of Adelaide).

1. Stress Orientations

In situ stress orientations were interpreted from 12 newly-analysed digital FMS/FMI image logs and 5 newly-analysed paper (S)HDT caliper logs. Furthermore, 20 stress orientations were compiled from pre-existing stress studies (Table 1). Digital image log data for 15 Cooper Basin wells were requested from Santos, however, none of these logs could be located internally requiring alternative sources to be found. The twelve digital FMS/FMI image logs analysed, were obtained from Schlumberger directly and a request for a further 8 wells remains with Schlumberger.

Tool	Format	Number of Wells	Data Source
Various/ Unknown	Text	20	Pre-existing internal Santos reports
FMS/FMI	Digital	12	Schlumberger
(S)HDT	Paper	5	Santos

Table 1 Summary of data acquired to date for Cooper Basin in situ stress map.

Stress magnitude modeling of the Three Queens area by David Campagna (consultant ARI) in April 2000, dictated the initial focus of stress orientation analyses. At that early stage in the ARC SPIRT project no image data had been located. Five paper (S)HDT caliper logs from the Three Queens area were retrieved from the Santos library and analysed for breakout occurrence.

The in situ stress map is shown in Figure 1 currently illustrates average stress orientations calculated from all observations made from available log intervals. Stress maps for

stratigraphic horizons of interest have not yet been prepared. However, the result database has been generated to permit easy map creation once all wells have been analysed (see §6 Results Database). All average stress orientations to date have been incorporated into DBmap for easy access and integration with the Santos database.

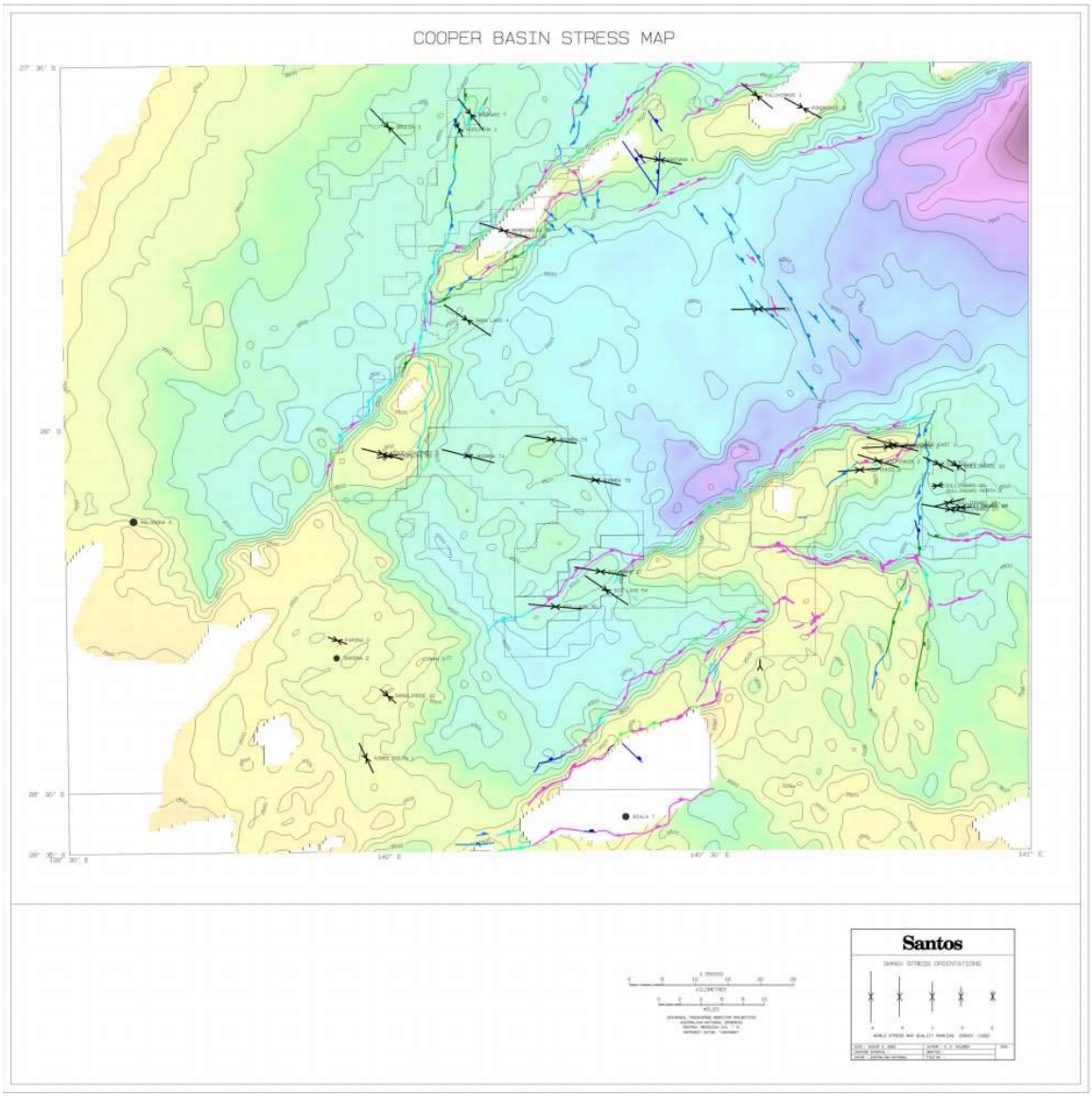

Figure 1 In situ stress map of the Cooper Basin. Long axes indicate Shmax direction and their length is weighted according to Zoback's (1992) World Stress Map ranking system.

The Cooper Basin Stress Map illustrates a consistent ≈ 100ºN σ_{Hmax} orientation in the Nappamerri Trough and rotates to a σ_{Hmax} orientation of ≈ 140ºN north of the GMI trend (Brolga-3, Moorari-7 and Woolkina-1) and ≈ 130ºN southwest of the Moomba Field (Farina-2, Koree South-1 and Daralingie-10). Further analyses in these areas will be performed to better constrain the rotation of the stress orientations.

No unequivocal stress rotations associated with faults have been observed.

Forward Program

A further 8 image logs will be analysed from across the Cooper Basin. Although the digital FMS/FMI data that has been requested from Schlumberger will provide the best coverage for the stress orientation map, the actual spread of data will be dictated by what data is ultimately obtained.

The stress orientation map will be updated in DBmap as analyses are completed. When all analyses are completed, horizon-specific stress orientation maps will be produced.

2. Stress Tensor

The in situ stress tensor has been determined for two areas in the Cooper Basin, dictated by the current focus of the LDG Task Force (Three Queens and Moomba). The stress tensor for other provinces in the basin will be determined as required by the LDG Task Force or as the distribution of available image log data is finalised.

The in situ stress tensor is defined using a suite of data, of which each component is determined using a separate technique (Figure 2). The current status of data acquisition and analysis of each component is listed below.

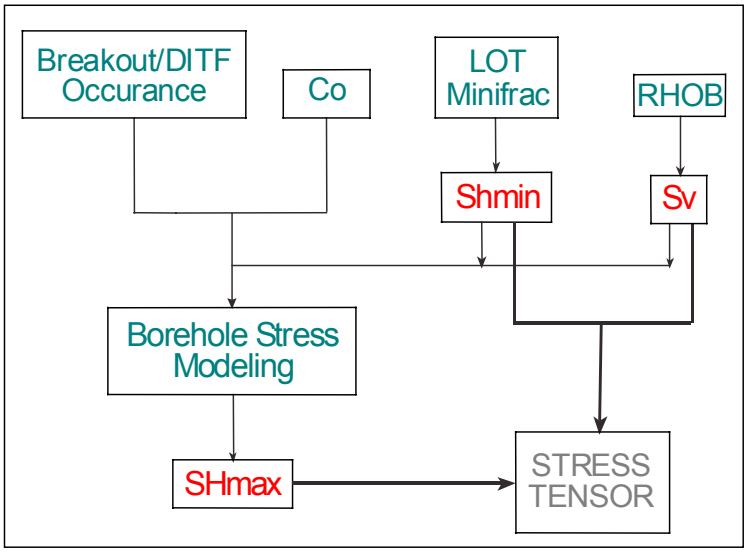

Figure 2 Flowchart illustrating component data and analyses that comprise in situ stress tensor determination.

Vertical Stress Magnitudes

No new vertical stress magnitude analyses have been undertaken as yet during the current phase of the project. Assessment of σ_v has relied upon previously determined stress gradients by Greenstreet (1999). Additional σ_v analyses will be performed after the distribution of available image log data is finalised.

Minimum Horizontal Stress Magnitudes

Compilation of leak-off tests (LOT's) and Minifrac data has commenced and is 80-90% complete. Assessment of the Three Queens and Moomba areas was performed using LOTs prior to the acquisition of the Minifrac data.

Preliminary assessment of the Minifrac data since has revealed that in the Moomba Province, depletion related changes to stress magnitudes are apparent and reassessment of the stress tensor will be required (Figure 3). It also indicates that depletion must be considered to successfully predict stress distribution and hence fracture 'sweet spots' across the Cooper Basin in any areas affected by depletion.

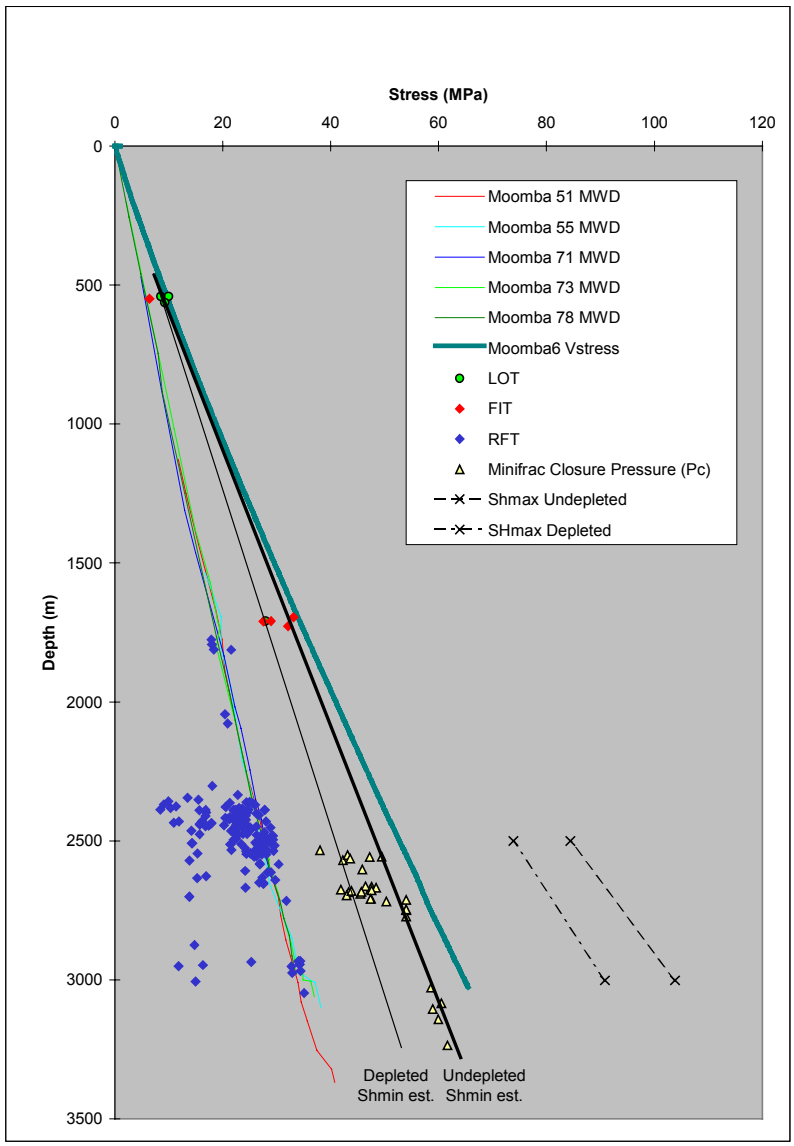

Figure 3 In situ stress tensor for the Moomba Province utilising minifrac data.

Maximum Horizontal Stress Magnitudes

The maximum horizontal stress magnitude (σ_{Hmax}) is estimated by modeling the borehole stresses to match the occurrence and non-occurrence of Breakouts and DITFs in the wellbore. Stress modeling of the wellbore is implemented using NCPGG developed specialist software, SWIFT (Stress Wellbore Interactive Failure Tool). Compressive rock strengths (Co) are critical to accurate constraint of σ_{Hmax}. Compilation of laboratory-derived rock strengths from across the Cooper Basin has begun and these results will be incorporated into σ_{Hmax} modeling, as they become available.

Forward Program

The stress tensor will be determined for areas dictated by the following variables:

- available image log data;
- Co and σ_v data coverage, and;
- requirements by the LDG Task Force.

Further analysis of the relationship between stress magnitude and reservoir pressure across the Cooper Basin will be undertaken.

Compilation of compressive strength data will be completed.

Additional σ_v magnitude calculations will be performed.

3. Fracture Analysis

The aim of fracture analyses for this phase of the ARC SPIRT project is to assess the distribution and type of fractures that are observed in image logs from the Cooper Basin. The fracture distribution is integrated with the in situ stress conditions to constrain fracture origin (natural or drilling induced). The relationship between fracture observations and stress conditions can be used to refine fracture 'sweet spot' predictions (Fracture Susceptibility).

Fracture Susceptibility

Fracture Susceptibility is the key methodology for identifying likely orientations of hydraulically conductive fractures or structural permeability networks. Given the in situ stress conditions the relative likelihood of fracture formation/reactivation can be assessed in terms of shear and normal failure mechanisms. For a given fracture orientation, the far field stresses can be resolved into shear and normal stress components acting upon that fracture. For all possible fracture orientations the relative probability of shear failure is directly proportional to the shear/normal stress ratio (Figure 4) and the relative likelihood of tensile failure is inversely proportional to the normal stress component (Figure 5). The likelihood of shear and tensile failure for all fracture orientations can be represented on a fracture susceptibility stereonet.

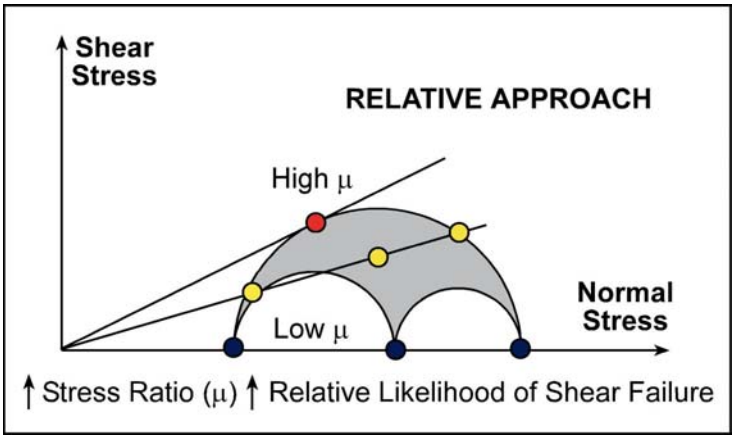

Figure 4 Relative likelihood of shear failure.

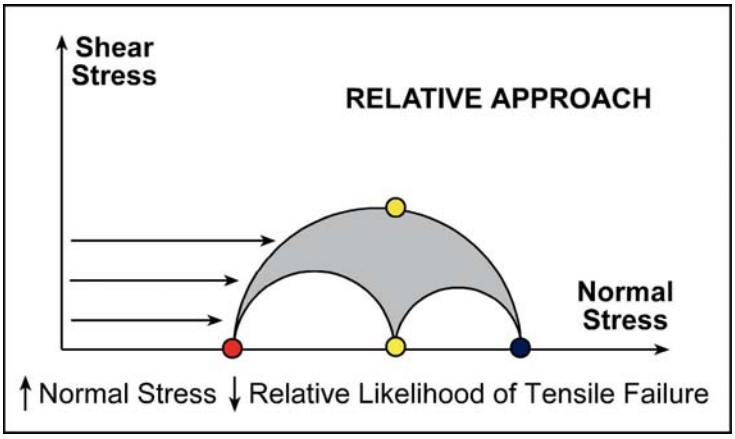

Figure 5 Relative likelihood of tensile failure.

Fracture susceptibility prediction for the Moomba Province has been assessed and is presented in Figure 6. The most likely orientation of open fractures with respect to the far-field stresses in the Moomba Province are those striking 060-140ºN and dipping greater than 60º to the north or south. The optimal drilling trajectory for open fracture intersection is a borehole deviated 60-90º towards 150-230ºN or 330-050ºN.

Fracture Susceptibility must be proven by comparison with fractures observed in the wellbore.

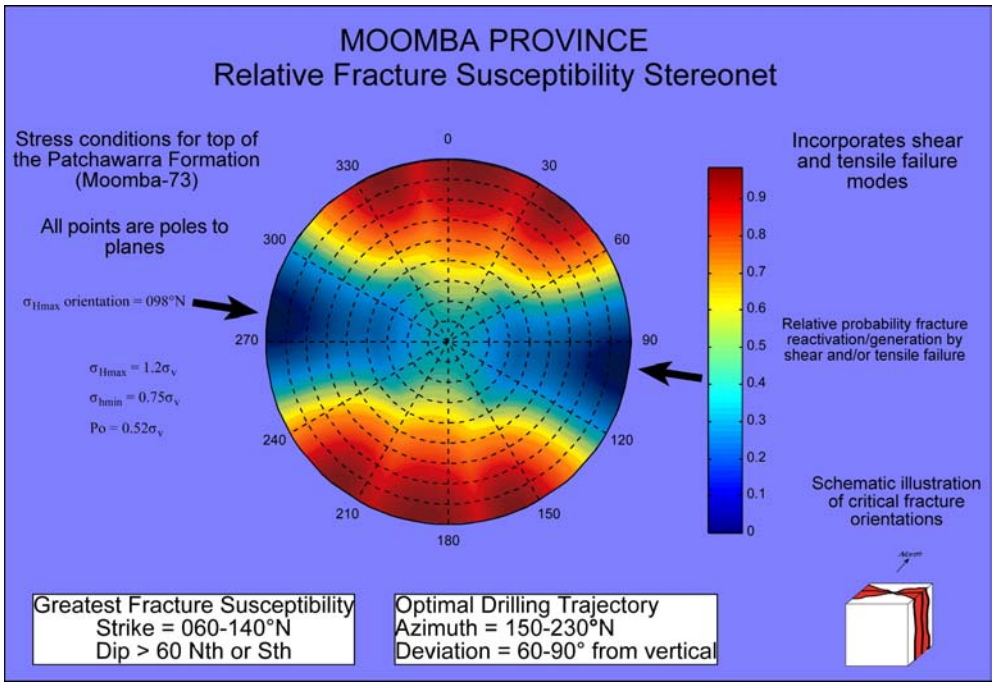

Figure 6 Preliminary fracture susceptibility stereonet for the Moomba Province calculated prior to availability of minifrac data.

Fracture Distribution

In addition to observing stress induced phenomena within resistivity images, fractures and faults are also interpreted. From 12 FMS/FMI image logs, 223 conductive fractures, 63 resistive fractures, 153 breakout-related fractures and 20 faults were interpreted. The distribution of conductive and resistive fractures is illustrated in Figure 7 and Figure 8.

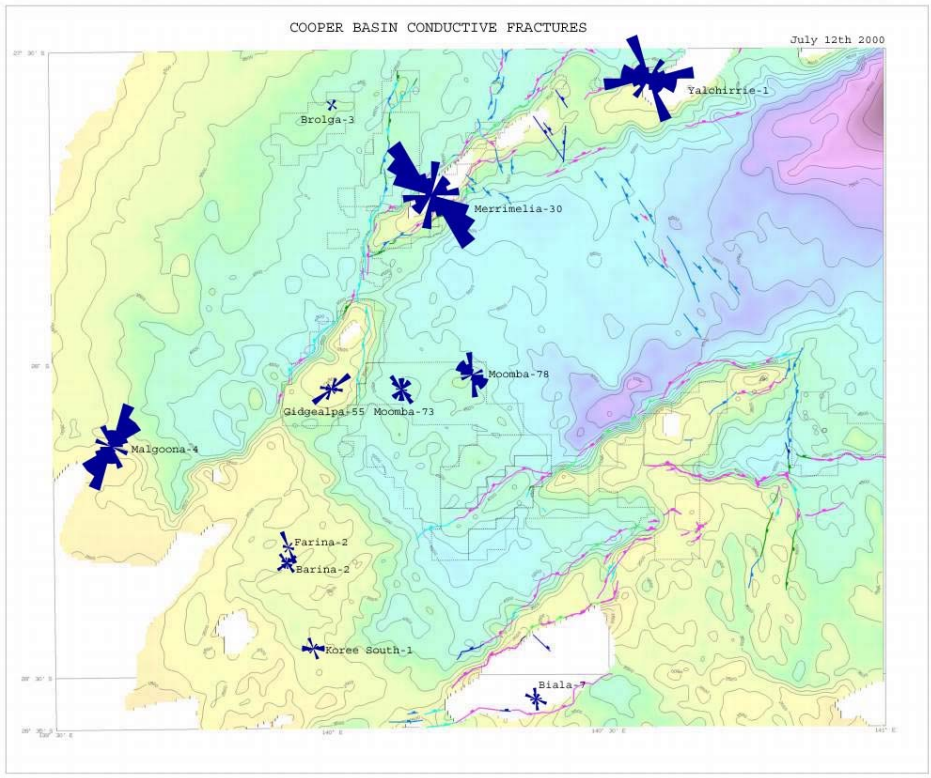

Figure 7 Map of conductive fracture distributions interpreted from resistivity logs in the Cooper basin. Rose petals are length weighted relative to fracture numbers, the longest representing 11 fractures. Note that fracture distributions are controlled by intervals of image log analysed and are not filtered for stratigraphy.

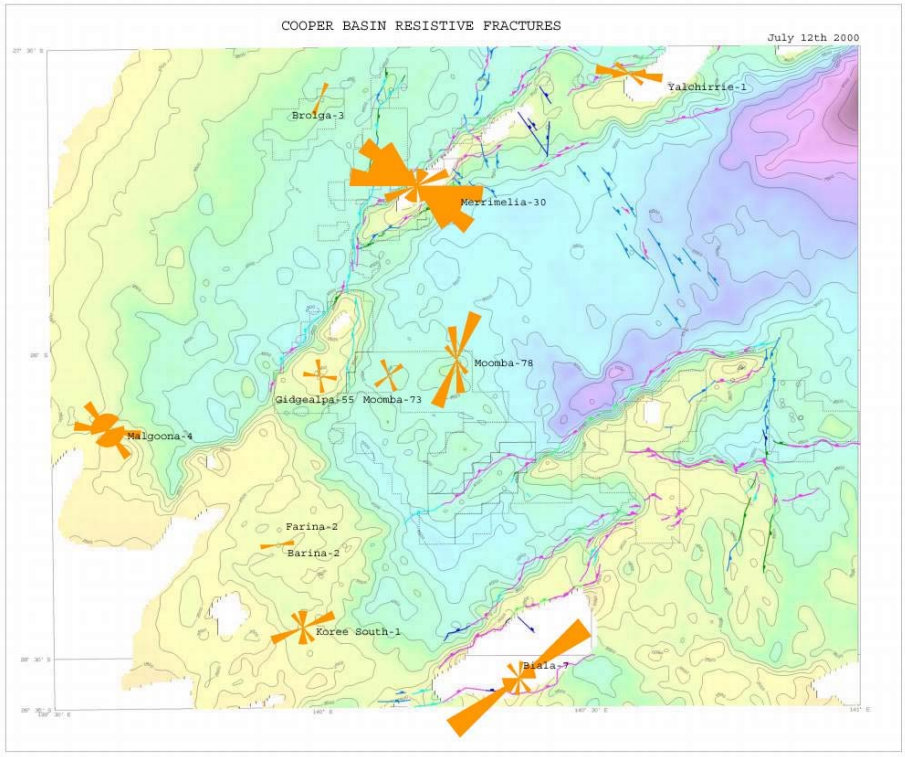

Figure 8 Map of resistive fracture distributions interpreted from resistivity logs in the Cooper basin. Rose petals are length weighted relative to fracture numbers, the longest representing 5 fractures. Note that fracture distributions are controlled by intervals of image log analysed and are not filtered for stratigraphy.

Conductive and resistive fracture populations for Moomba-73 have been plotted on a 3D Mohr circle defined by the far field stresses of the Moomba Province (Figure 9). A conductive fracture is interpreted to be an open natural fracture and a resistive fracture is interpreted to be a closed natural fracture. Open fractures are expected to be critically oriented with respect to the stress regime and have a high fracture susceptibility. Closed fractures are not expected to be critically oriented and have a low fracture susceptibility.

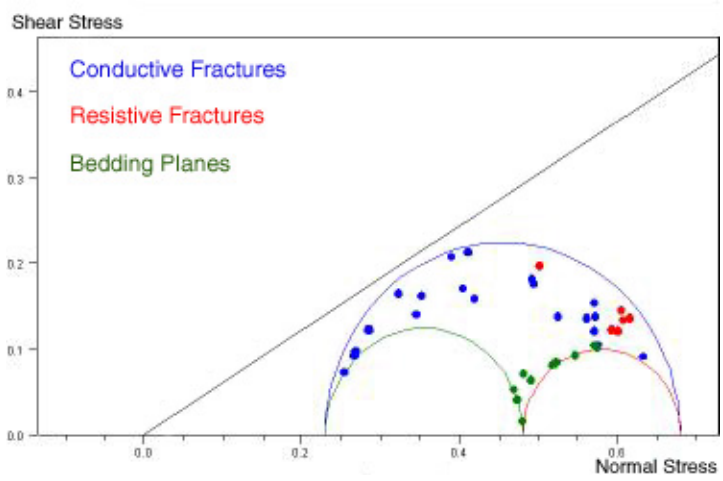

Figure 9 Three dimensional Mohr circle representing the far field stress conditions in the Moomba area (prior to minifrac data) with conductive and resistive fracture populations plotted in terms of shear and normal stress components.

Comparison of various fracture types interpreted from the Moomba-73 well with the predicted fracture susceptibility for the Moomba Province are shown in Figure 10. Resistive fracture orientations in Moomba-73 correspond to predicted orientations of low fracture susceptibility and the orientations of the majority of conductive fractures correspond to high fracture susceptibility. However, a small population of conductive fractures also corresponds to a low fracture susceptibility. This population is suspected to represent fractures that are open at the wellbore due to the near wellbore stress distribution and are not expected to be open away from the wellbore. Further modeling of wellbore stresses will be implemented to differentiate between far-field (natural) conductive fractures and near wellbore (drilling induced) conductive fractures.

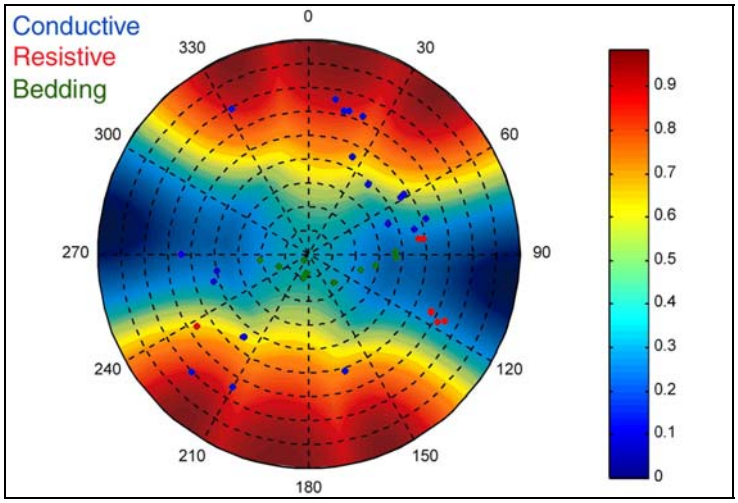

Figure 10 Comparison of fracture orientations by fracture type and the predicted fracture susceptibility.

Forward Program

Detailed well card summaries that present all aspects of interpretation for a particular well (fractures, stresses, image interpretation intervals) with stratigraphy for inter-well comparison.

Fracture distribution maps by stratigraphic horizon.

Integration of fracture types with in situ stresses as stress tensors are determined.

Fracture susceptibility assessment across Cooper Basin.

4. Overpressure Analysis

Pore pressure analysis is an important aspect of the stress tensor. The occurrence of non-hydrostatic pore pressures influences the distribution of open natural fractures. The pore pressure part of the project focuses on compiling observed pore pressure data (mud weights, drill stem tests, and wireline formation interval tests), and inferring pore pressures from wireline logs.

Observed Pressure Data

Initial well selection has taken place based on proximity to the Nappamerri Trough, well coverage surrounding the well, the depth of the well and the amount of pressure data available for each well.

Wireline Log Analysis

Wireline log analysis will take place on a subset of the wells included in the Observed Pressure Data study. Initial wireline log analysis applied the Eaton quantitative pressure method to the sonic log in Swan Lake-1, Wantana-1 and Strathmount-1. The pressure profile from Strathmount-1 is shown in Figure 11.

Forward Program

Pore pressure data will be compiled and included in the Result Database. Occurrences of overpressure will be mapped out and the vertical and horizontal extent of the overpressure will be estimated.

Wireline log analysis will be performed on a sub-set of the wells in the database. Eaton pressure analysis (DT only), conversion to porosity (RHOB, DT, NPHI), and the resistivity logs will also be analysed. Pressure estimates resulting from the wireline log analysis will be included in the Results Database (See §5).

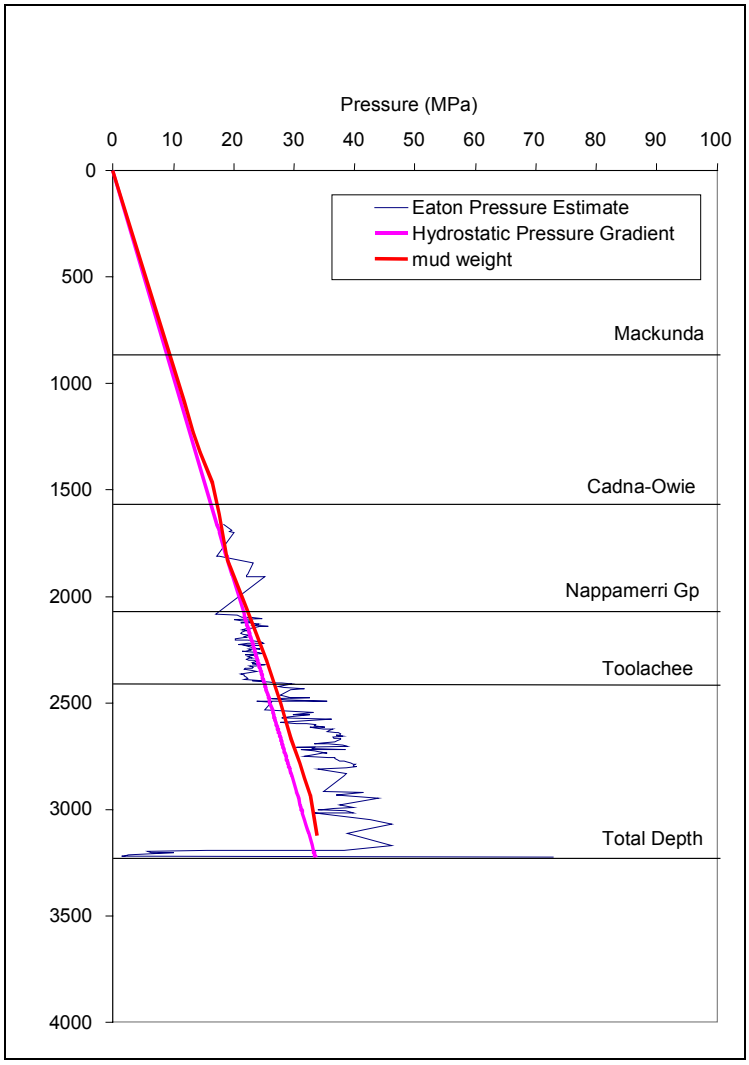

Figure 11 Strathmount-1 Eaton Pressure versus depth. Mud weight, and hydrostatic gradient have also been plotted.

5. Results Database

The results database is a Microsoft Access repository for all interpretation data and information pertaining to the ARC SPIRT Project. Although not originally specified as a project deliverable, the database will dramatically aid the production of other deliverables and provide technology transfer at the conclusion of the project. Other advantages of the database include:

- one repository for all analyses related to the project including stress data, fracture types, resistivity images, reports and basic well information;
- easily accessible results that can be exported in table format (Excel or similar);
- integrated with stratigraphy (lithostratigraphic and chronostratigraphic) in order to assess results by horizon;
- powerful data retrieval, and;
- delivered on a CD at the conclusion of the project.

Forward Program

Updates to the result database are ongoing and new features are added as they are required to meet other project deliverables.

Program for Remainder of 2000

1. *Image Analysis*
   - Dependent on request for 8 wells remains outstanding with Schlumberger
   - Observation of in situ stress features and fracture populations from 8 FMS/FMI image logs.

2. *Stress Tensor*
   - Calculation of additional σv gradients.
   - Assess relationship between Minifrac closure pressures (Pc) and reservoir pressures (Pf).
   - Depletion distribution.
   - Compile compressive rock strength data.
   - Maximum horizontal stress modeling for stress provinces across the Cooper Basin.

3. *Fracture Analysis*
   - 3D Mohr assessment of fracture populations.
   - Natural vs. drilling induced fracture populations.
   - Fracture Susceptibility prediction across Cooper Basin.
   - Integrated well data cards.

4. *Maps*
   - Continue to update σ_{Hmax} orientation map.
   - σ_v σ_{hmin} and σ_{Hmax} gradient maps.
   - Depletion distribution?
   - Distributions of conductive and resistive fracture populations.
   - Overpressure distribution.

5. Overpressure

- Compilation of observed pressure data
- Wireline log analysis based on sonic log, density log, neutron porosity logs, and resistivity logs.
- Input on the size of velocity anomaly associated with overpressured sediments

6. Stress Modeling

- In collaboration with Tony Meyers, Uni of SA.